Doctoral　Thesis

博士論文

Investigation of immune checkpoint CD200-CD200R axis within non-small cell lung cancer (非小細胞肺癌における免疫チェックポイント CD200 - CD200R axis の検討)

蘇　英晗

Index

Abbreviations

Bovine serum albumin (BSA)

Cancer-associated fibroblasts (CAFs)

Cell surface transmembrane glycoprotein CD200 receptor (CD200R)

Cluster of Differentiation 200 (CD200)

Cluster of differentiation 3 (CD3)

Cluster of differentiation 4 (CD4)

Cluster of differentiation 8 (CD8)

Cluster of differentiation 14 (CD14)

Cluster of differentiation 20 (CD20)

Cluster of differentiation 28 (CD28)

Complementary deoxyribonucleic acid (cDNA)

Cyclin-dependent kinase 4 (CDK4)

Cytotoxic T lymphocyte-associated protein 4 (CTLA-4)

Deoxyribonucleic acid (DNA)

Dri tumor & tissue dissociation reagent (TTDR)

Dulbecco's modified Eagle's medium (DMEM)

Ethylenediaminetetraacetic acid (EDTA)

Extracellular matrix (ECM)

Fetal bovine serum (FBS)

Fluorescence-activated cell sorting (FACS)

Genomic deoxyribonucleic acid (gDNA)

Hepatitis A virus cellular receptor 2 (HAVCR2)

Human telomerase reverse transcriptase (hTERT)

Immune checkpoint molecules (ICs)

Immune checkpoint inhibitors (ICIs)

Indoleamine-pyrrole 2,3-dioxygenase (IDO)

Interferon-gamma (IFN-γ)

Interleukin 4 (IL-4)

Interleukin 6 (IL-6)

Interleukin 10 (IL-10)

Interleukin 12 (IL-12)

Interleukin 13 (IL-13)

Lymphocyte-activation gene 3 (LAG-3)

Magnetic-activated cell sorting (MACS)

Messenger ribonucleic acid (mRNA)

Minimum Essential Medium Eagle - alpha modification (α-MEM)

Mitogen-activated protein kinase (MAPK)

Non-small cell lung cancer (NSCLC)

Peripheral blood mononuclear cells (PBMCs)

Phosphate-buffered saline (PBS)

Programmed cell death protein 1 (PD-1)

Propidium iodide (PI)

Pulmonary artery (PA)

Ribonucleic acid (RNA)

Real-time polymerase chain reaction (RT-PCR)

Roswell park memorial institute medium (RPMI1640)

Short hairpin ribonucleic acid (shRNA)

T-cell immunoglobulin and mucin-domain containing-3 (TIM-3)

T cell immune-receptor with Ig and ITIM domains (TIGIT)

Transforming growth factor-beta (TGF-β)

Tumor-infiltrating lymphocytes (TILs)

Tumor microenvironment (TME)

Tumor necrosis factor-alpha (TNF-α)

(A.) Introduction

Tumor is a chaotic complex, which is including not only cancer cells but also stromal cells, tumor-infiltrating immune cells and extracellular matrix (ECM). The interactions between those various components are playing key roles in sharping hallmarks of cancer, and also have a huge influence on outcomes of cancer therapies [1, 2]. For the past few decades, increasing numbers of studies have been focused on this so-called tumor microenvironment (TME). As one of the most abundant stromal cell types within TME, cancer-associated fibroblasts (CAFs) were widely reported about their important roles in tumor progression, therapeutic process, and also their potential as therapeutic targets [3-6]. As non-professional antigen-presenting cells, CAFs are reported to produce different kinds of cytokines to influence the immune balance within tumor tissue [7-10]. Beyond indirect cell-cell interaction in shaping a tumor-favor immune microenvironment, studies have shown that CAFs may also present immune checkpoint molecules to directly suppress tumor infiltrating immune cells [9-11].

Based on a further understanding in both immunology and TME, the discovery of immune checkpoints has proven to be one of the most important advancements for cancer therapy development. Immune checkpoints are the key molecules that act as brakes to restore immune homeostasis after diseases, and those molecules are hijacked by cancer cells to inhibit immune activities. The currently most well studied checkpoints are programmed

cell death protein 1 (PD-1) and cytotoxic T lymphocyte-associated protein 4 (CTLA-4). Immune checkpoint inhibitors (ICIs) have already been administered as first-line treatments for advanced-stage non-small cell lung cancer (NSCLC) patients. Compared with standard chemotherapy, ICIs have led to promising, durable responses and exhibited possible benefits for long-term survival [12, 13].

CD200R and its ligand, CD200, have also been reported to be functional immune checkpoints. To date, it is well documented that the interaction between CD200 and CD200R triggers an immune suppression signal to inhibit the RAS/MAPK signal cascades, resulting in a decrease in the production of inflammatory cytokines and an increase in the anti-inflammation cytokine secretion [14-18].

The potential of CD200-CD200R has been widely discussed in the context of diseases or therapies related to the immune system, such as arthritis, infection and transplantation [19-21]. Many previous studies have claimed that CD200 expressed by cells of melanoma, ovarian cancer, breast cancer and hepatocellular carcinoma, can interact with CD200R, which is a prognosis factor or even a biomarker for cancer stem cells [22-25]. Meanwhile, CD200R was reported as a prognosis factor in lung cancer, and high stromal CD200R expression was strongly connected with non-adenocarcinoma histological types (e.g., squamous cell carcinoma and other subtypes), and also with advanced disease stage [26].

The expression of CD200R is restricted to the surfaces of immune cells, such as

monocytes, macrophages, neutrophils and dendritic cells from the myeloid lineage and T cells and B cells from the lymphoid lineage [14-16, 27]. On the other hand, CD200 is reported to be widely distributed among cells of both hematopoietic and non-hematopoietic origins, such as neurons, endothelial cells, fibroblasts, and multiple types of cancer [28-31].

Although ICIs have already achieved a great achievement in treatments of several types of cancer, there are still certain ratios of patients who show no response to ICI therapy. Investigations in reliable biomarker and novel checkpoints are intensely required in order to enhance the efficacy of ICIs. In this study, we attempted to investigate the distribution of CD200 and CD200R within NSCLC and also test the function of this axis with a co-culture system. Various expression of CD200R between T cells extracted from tumor tissue and T cells from dissected lung pulmonary artery (PA) blood were confirmed. At the same time, co-expression of CD200R with three other immune checkpoint molecules, PD-1, CTLA-4 and TIM-3, were also found within tumor infiltrating T cells.

(B.) Investigation of CD200-CD200R axis between CAFs and immune cells

I. Aim

Checking the genericity of CD200-expressing CAFs within NSCLC

Identifying immune cells expressing CD200R within NSCLC

Investigating functions of CD200-CD200R axis between CAFs and immune cells

II. Results

1. *Investigation of CD200 RNA and protein expression within CAF library*

In order to confirm the genericity of CD200-expressing CAFs among NSCLC patients, we investigated CD200 mRNA and surface protein expression level with quantitative real-time polymerase chain reaction (qRT-PCR) and fluorescence-activated cell sorting (FACS) analysis among our pre-established CAF library [32, 33]. Among 19 cases of CAF samples, 6 samples have shown mRNA expression of CD200 (shown in Fig. 1A), with sample 608 taken as the positive control, which was the case reported in our previous study [28]. For FACS analysis, 4 samples were classified as positive samples with surface expression of CD200 higher than 5% among entail populations (shown in Fig. 1B; Supplementary Fig. S1A, S1B, S1C). Taking together, 4 cases among 19 CAF samples were constantly express CD200 at both mRNA and membrane protein levels, which confirmed that CD200-expressing CAFs are not a single case report. The pathological characteristics of these 19 cases were also taken into investigated, which has shown no significant correlation with any common characteristics (shown in Table. 1).

2. *Life extension and construction of CD200 overexpress and shRNA knockdown CAF cell lines*

As the primary culture cells have a limited life span, life extension of picked-up

CAF strains was conducted with lentivirus-mediated gene transfer of human telomerase reverse transcriptase (hTERT) and a mutant form of cyclin-dependent kinase 4 (CDK4R24C). Successful transfection of hTERT and CDK4 was confirmed with both fluorescence and RT-PCR (shown in Fig. 2A; Supplementary Fig. S2A). Sample 1228 is considered as a negative sample which was transfected with over-expression vector, and 721pm is considered as the most positive sample, which was knocked down with shRNA. The establishment of CD200 overexpress and shRNA knockdown CAF cell lines were confirmed with FACS analysis (shown in Fig. 2B, 2C; Supplementary Fig. S2B).

3. Investigation of CD200R expression within tumor-infiltrating leukocytes in NSCLC

To confirm whether the expression of CD200R is mainly limited to cell populations of the myeloid lineage, tumor-infiltrating leukocytes were collected through the enzymatic digestion of dissected tumor specimens for flow cytometry analysis (shown in Fig. 3A, 3B; Supplementary Fig. S3). Among the infiltrating immune cells, CD3+ T cells accounted for an average of 46.55% of all the extracted cells (shown in Fig. 3B, 3C), which was significantly higher than the proportions of monocytes (CD14+; 11.94%) and B cells (CD20+; 17.61%). In addition, CD200R was expressed on the surface of 70.52 % of CD3+ T cells (shown in Fig. 3D), and this expression was significantly higher than that of CD14+ cells (46.64%) and CD20+ cells (61.00%).

4. *Investigation of CD200R expression within peripheral blood mononuclear cells (PBMCs) extracted from pulmonary artery (PA) blood*

Next, peripheral blood mononuclear cells (PBMCs) were collected from the pulmonary artery (PA) blood of resected lung specimens, and a similar proportion of CD200R+ cells were observed; of these CD200R+ cells, T cells were most abundant among the extracted immune cells (shown in Fig. 4A, 4B; Supplementary Fig. S4A). In contrast to tumor-infiltrating T cells, only 55.06% of CD3+ T cells extracted from PA blood were found to have CD200R expression (shown in Fig. 4B, 4D). To further characterize CD200R+ T cells, magnetic-activated cell sorting was conducted to purify CD3+ T cells from all PBMCs, to evaluate the expression levels of CD200R on CD4+ and CD8+ T cells (shown in Fig. 4C; Supplementary Fig. S4B, S4C, S4D). As Figures 4D and 4E show, both CD4 (73.71%) and CD8 T (66.05%) cells expressed CD200R.

5. *Construction of the co-culture system and check for CD200-CD200R axis interaction between CAFs and immune cells*

To investigate the CD200-CD200R axis, a co-culture system has been constructed, which the expanded T cells (extracted from PA) were seeded into culture dishes with either CD200-negative or CD200-positive CAFs (shown in Fig. 5). After 48 hours of co-culture, T cells were collected for downstream assays by centrifugation of supernatant

of the co-culture system. Similar co-culture system was applied to myeloid cell lines THP-1 and U937 (shown in Supplementary Fig. S5).

The cytokine expression pattern was first checked with RT-PCR to confirm the influence of interactions between CAFs and T cells. However, neither pro-inflammatory cytokines (Interferon-gamma: IFN-γ; Tumor necrosis factor-alpha: TNF-α) nor anti-inflammatory cytokines (Transforming growth factor-beta: TGF-β, Interleukin 4: IL-4, IL-10 and IL-13) expressed by T cells have shown a significant difference between co-culture with CD200-negative or CD200 overexpressed CAFs (shown in Fig. 6A; Supplementary Fig. S6A). Although THP-1 cell line has shown downregulation of IL-6 after co-culture with CD200-expressing CAFs, a similar phenomenon was not found with U937 cell lines (shown in Supplementary Fig. S6B, S6C).

For the functional assay, T cell apoptosis levels were checked with Annexin V and propidium iodide (PI) staining by FACS analysis, which no significant differences of apoptosis or necrosis levels were found among 3 samples (shown in Fig. 6B).

To further confirm the interaction between CD200 and CD200R, the recombinant CD200 protein was added into the culture medium of T cells in different concentration from 0 to 100 ng/mL. No dose-dependent pattern of cytokine expression was observed (shown in Fig. 7A; Supplementary Fig. S7A). In addition, a blocking antibody of CD200R (50 μg/mL) was added into medium of the co-culture system so as to interfere

with the CD200 and CD200R interaction between cells. As showed in Figure 7B, the up-regulation of IL-4 cannot be cancelled by introducing a CD200R-blocking antibody. Similarly, the downregulation of IL-6 observed in THP-1 cell line also cannot be neutralized with a CD200 blocking antibody (30 μg/mL) or CD200R knock-down (shown in Supplementary Fig. S7B).

III. Discussion

The previous study from our group confirmed the existence of a subpopulation of CAFs with CD200 expression within one single case. Through checking CAF library which was pre-established within our lab, CD200+ CAFs were found about roughly 20-25% in NSCLC samples.

Surprisingly, despite most of the previous studies focused on CD200R expression among myeloid-lineage cells, our result indicated that TILs were dominated with CD200R-expressing T cells. This suggested that CD200R may potentially not only participate in the innate immune response but also have a role in the adaptive immune response. Further study of this dual characteristic of CD200R is required.

Unfortunately, the attempt to prove any direct cell-cell interaction or molecule interactions between fibroblasts and immune cells were failed. It is predicted that the efficiency of interactions between adhesion cell lines (CAFs) and suspension cells

(immune cells) was not reproducible within this co-culture system. In addition to that, the heterogeneity of extracted T cells may also contribute to the complex results, as components varied from patient to patient. The established co-culture system was not suitable to confirm or ensure the interaction among CD200-expressing CAFs and CD200R-expressing immune cells, which was one of the main limitations of this study. Lacking in commetially available antibodies for phosphorelated CD200R and several downstream proteins also restrained our options for inspectation.

For revealing the interaction of CD200-CD200R axis within tumor tissue, the better approach might be to construct an in vivo model or an ex vivo model, such as a mouse or organoid model. Both mouse model and organoid model were aiming to stimulate a more vivid tumor microenvironment in comparison to traditional 2D culture. It is predicted that a more compact, solid vivo model may provide us with a chance of direct cell-cell interaction.

(C.) Investigation of CD200R and multiple immune checkpoint molecules among T cells in NSCLC

I. Aim

Investigation the difference of CD200R expression between the PA blood cells and TILs and their various in immune checkpoint profiles.

II. Results

1. *A higher proportion of CD200R expression in tumor-infiltrating T cells compared with peripheral blood T cells*

To further confirm the differences in CD200R expression between tumor-infiltrating T cells and PA blood-derived T cells, MACS-sorted CD3+ T cells from paired PA blood and TIL samples (shown in Fig. 8A, 8B) were analyzed. Twelve samples of T cells showed that tumor-infiltrating T cells were dominated by CD200R+ T cells, compared to peripheral blood T cells (shown in Fig. 8A). Moreover, similar results were obtained in 3 paired samples of PA blood and tumor tissue (shown in Fig. 8B). On the other hand, CD8+ cells tend to be the main reason for this increase in the CD200R+ population (shown in Supplementary Fig. S8A), while those numbers in CD4+ cells might differ from sample to sample (shown in Supplementary Fig. S8B).

2. *Co-expression of CD200R and multiple immune checkpoints*

Given that CD200R is an immune checkpoint which regulates immune cell activity, we investigated cells collected from the paired PA blood and tumor specimens by FACS analysis, to determine whether other immune checkpoints may be upregulated and co-expressed with CD200R. An average of 52.02% of tumor-infiltrating T cells expressed both PD-1 and CD200R (shown in Fig. 9A, left). In comparison, only an average of

23.21% of T cells extracted from PA blood expressed both PD-1 and CD200R. Similarly, co-expression of PD-1 and CD200R was also significantly increased among CD4+ (1.61-fold) and CD8+ (1.79-fold) T cells when comparing T cells derived from PA blood and those derived from tumor tissue (shown in Fig. 9A right; Supplementary Fig. S9A, S9B, left; S9C, S9D). For CTLA-4 and TIM-3, both of these checkpoints showed a limited level of expression on the surface of CD3+ T cells derived from PA blood (CTLA-4: 1.19%; TIM3: 0.89%; shown in Fig. 9B, 9C, left). Among tumor-infiltrating T cells, CTLA-4 was co-expressed with CD200R on 21.88% of CD4+ T cells and 20.75% of CD8 cells, which was significantly up-regulated compared to paired PA samples (shown in Fig. 9B, 9C; Supplementary Fig. S9A, S9B, middle and right). Moreover, as Figure 3C shows, co-expression of TIM3 and CD200R was limited to CD8 T cells and showed differences between the PA and TIL samples.

3. *A high level of immune checkpoint expression in the CD200R-high group confirmed by public database*

To confirm that the co-expression of CD200R and other immune checkpoints can be generalized to a wider population, an analysis of a TCGA lung adenocarcinoma database was introduced into this study. Based on the median CD200R mRNA (CD200R1) expression level, 517 samples were separated into the CD200R-high and CD200R-low

groups (or the CD200-high and CD200-low groups). The mRNA expression levels of 6 immune checkpoints, including PD-1 (PDCD1), CTLA-4, TIM-3 (HAVCR2), lymphocyte activation gene 3 (LAG-3), T cell immune-receptor with Ig and ITIM domains (TIGIT), indoleamine-pyrrole 2,3-dioxygenase (IDO1), and the correlations of these molecules with CD200R1 were investigated. All six immune checkpoints showed significantly higher expression levels in the CD200R-high group (shown in Fig. 10 and Fig. 11). At the same time, the other immune-related genes also have shown a similar tendency (shown in Supplementary Fig. S10). As shown in Supplementary Fig. S11, the correlation of CD200 and CD200R mRNA expression, the overall survival and disease-free survival were also investigated.

III. Discussion

In this study, we demonstrated that CD200R was highly expressed in tumor-infiltrating T cells in NSCLC, and CD200R was highly co-expressed with multiple immune checkpoints. Most studies only focused on CD200R expression and its function among myeloid lineage cells [16, 18, 29]. However, our results demonstrated that both B cells and T cells express CD200R. Based on the current model of the cancer-immune cycle [34], those T cells collected from cancer patients PA were recruited from nearby lymph nodes and were activated by antigen-presenting cells. The PA blood used in the

experiments was considered to be the inflow tract into the lung tissue, delivers blood circulating immune cells into the tumor. The significant differences of the immune checkpoint profile between the inflow tract of PA blood and accumulated tumor-infiltrating immune cells suggested that significant changes to their phenotype may have happened, and these changes might be due to the changes in the surrounding microenvironments, which also reinforced by the results of public database analysis.

It is well reported that most tumor-infiltrating T cells have entered the stage of exhaustion or dysfunction [35]. Many studies have confirmed that the exhausted or dysfunctional T cells simultaneously express multiple immune checkpoints, including PD-1, CTLA-4, TIM-3, LAG-3 and TIGIT [36-39]. Different levels of checkpoint co-expression represent highly heterogenic T cell populations with different stages of exhaustion, for example, a subpopulation of T cells with expressing both of PD-1 and TIM-3 was well reported as a terminal exhausted group with no polyfunctionality retained [40-42]. It is widely accepted that before T cells differentiated into the terminal exhausted stage, dysfunction of T cells might be refined through the introduction of ICIs, such as anti-PD1 [43, 44], which can tip the balance of immune microenvironments from cold (inhibitory) to hot (activating). One of the previous studies claimed that CD4 T cells increased CD200R expression level and loss of multifunctional potential during chronic infection [45], which might have happened similarly inside tumor tissue. The fact that

CD200R is also largely co-expressed with other checkpoints inside tumor suggests that tumor-infiltrating T cells have entered the exhaustion stage. A combination of CD200R and other checkpoints might be able to act as biomarkers, which can specify a subgroup of T cells with a certain level of exhaustion. Furthermore, combinational blockage strategies of multiple immune checkpoint molecules have been designed aiming to broaden the horizon for ICIs [46-49], targeting CD200R together with other checkpoints could be a promising candidate to restore T cell activities. Although checkpoint molecules were known to have a completely different mechanism, which requires a further detailed study of CD200-CD200R axis pathway. Currently, An inhibitor of CD200 has entered into a clinical trial for chronic lymphocytic leukemia and multiple myeloma [50], the results of a lung cancer study claimed that CD200 might be a favorable prognostic factor [26]. Moreover, our previous study has indicated that CD200 might potentially augment cancer cell sensitivity to chemotherapy [28, 51], which suggested that CD200 may potentially have functions other than immune modulation.

(D.) Conclusion

In conclusion, our research investigated the expression level of a pair of immune checkpoint molecules, CD200 in CAFs, and CD200R in PA blood and TILs within NSCLC. The CD200-expressing CAFs were confirmed more general than one rare single

case. However, our attempt to confirm the interaction between CAFs' CD200 and CD200R expressed on the surface of either T cells or myeloid cell lines were failed, presumably due to the unreliability of our established co-culture system.

On the other hand, the tumor-infiltrating T cells were found to be more strongly dominated by CD200R expressing T cells, compared to the T cells from PA blood. Moreover, the expression of CD200R largely overlapped with that of other immune checkpoints, including PD-1, CTLA-4 and TIM-3. Considering this finding, co-expression of CD200R and other immune checkpoints might be a good biomarker of T cell phenotypic changes or even a potential target for immune-therapy.

Considering the main limitation of our study, an urgent request for future study would be constructing a more reliable vivo model as aforementioned. Introducing a stabilized model will be helpful for downstream metabolic analysis, epigenetic studies or transcriptomic study that may further elucidate the subpopulations of CD200R+ T cells and exhausted cells. For example, a transcriptomic analysis of high, intermediate and no or low CD200R expression might give us a better view of the big picture of T cell states, similar to the previous study [43]. Based on the constructed model and results of downstream assays, testes of administrating of immune checkpoint inhibitor would also be an option, which can further elucidate the molecular mechanism of CD200-CD200R axis and their potential of being biomarkers or drug targets.

(E.) Materials and Methods

1. Cell culture

The human monocytic cell lines THP-1 and U937 were received as gifts from the Division of cancer immunotherapy (Dr. Yasushi Uemura). The primary culture of CAFs was established in previous studies from samples [32, 33], which were obtained from surgically resected lung tissue at National Cancer Center Hospital East.

The THP-1 and U937 cells were maintained in Roswell park memorial institute medium (RPMI1640; Sigma-Aldrich, Missouri, United States) supplemented with 10% fetal bovine serum (FBS; Life Technologies, California, United States), 1% Penicillin Streptomycin (Sigma-Aldrich). T cells were maintained in RPMI1640 supplemented with 10% FBS, 1% Penicillin Streptomycin and IL-2 (BioLegend, California, United States). CAF cells were maintained in Minimum Essential Medium α (MEM-α; Gibco, Langley, United States) with 10% FBS and 1% penicillin and streptomycin. All cells were incubated at 37 °C in a humidified atmosphere containing 5% CO_2.

2. Lentivirus-mediated gene transfer

For life extension of CAFs, lentiviruses were provided by the HEK293T cells co-transfected with CSII-CMV-RfA-IRES2-Venus plasmid containing hTERT [32], CSII-CMV-RfA-IRES2-Venus contain CDK4R24C [33], packaging vector

pCMV-VSV-G-RSV-Rev (RIKEN BioResource Center, Tsukuba, Japan), and packaging vector pCMV-HIV (RIKEN BioResource Center), using Lipofectamine 2000 transfection reagent (Invitrogen, California, United States.) according to the manufacturer's instructions. Vector-containing medium was filtered through a 0.45-μm filter (Merck Millipore, Massachusetts, United States), and 8 μg/mL of polybrene (Santa Cruz Biotechnology, Texas, United States) was added for target cell transduction. Detailed procedures and mechanism were fully explained in our prvious study [32]. The fluorescent signal of Venus proteins was observed by fluorescence microscope (shown in Supplementary Fig. S2).

3. Construction of shRNA with LR recombination

To create entry clones, the top and bottom strands of each CD200R shRNA oligonucleotide were annealed and ligated into pENTR4-H1 (RIKEN BioResource Center). Thereafter, LR recombination reactions were performed between the entry clones and CS-RfA-EG (RIKEN BioResource Center) using Gateway LR Clonase (Thermo Fisher Scientific, Massachusetts, United States). Lentiviruses were produced using HEK293T cells co-transfected with packaging constructs pCAG-HIV, pCMV-VSV-G-RSV-Rev and vectors containing CD200R shRNA or control vector containing luciferase. Infection was achieved as aforementioned. Stable transformants

of CD200R knocked down THP-1 cells were confirmed with a FACS Accuri C6 plus (BD Biosciences, New Jersey, United States). The sequence of used shRNA was listed in Supplementary Table S2, and all vectors used were shown in Supplementary Fig. S12.

4. Tumor-infiltrating leukocytes (TILs) extraction

Human lung specimens were obtained from the surgically resected lung tissues of non-small cell lung cancer (NSCLC) patients at National Cancer Centre Hospital East. This retrospective study was approved by the National Cancer Ethical Review Board (IRB approval number; 2005-043). De-identified tissue specimens were received by research staff directly after the surgeries. The tissue specimens were plated on a culture dish containing Dulbecco's Modified Eagle Medium (DMEM: Sigma-Aldrich) and cut into small pieces with sterilized scissor and tweezer. The minced specimens were then transferred to a 50-mL centrifuge tube with pre-prepared BD Horizon™ Dri Tumor & Tissue Dissociation Reagent (TTDR; BD Biosciences) according to the manufacturer's instructions. The mixture was placed in a 37°C water bath for 30 minutes with frequent agitation until the tissue was enzymatically dissociated into a single-cell suspension. The enzymatic reaction was stopped by washing with phosphate-buffered solution (PBS; Sigma-Aldrich) with 1% bovine serum albumin (BSA; Life Technologies) and

ethylenediaminetetraacetic acid (EDTA; final concentration 2mM; Sigma-Aldrich). The cell suspension was pooled with the stored supernatant and filtered through a 70-μm filter (Corning Inc. New York, United States). After centrifugation at 300g for 10min, the pelleted samples were treated with 2mL 1x BD Pharm Lyse Buffer (BD Biosciences) for 15min at room temperature to remove the erythrocytes. The reaction was neutralized with 40 mL PBS containing 1% BSA and 2mM EDTA. After centrifugation at 300g for 10min, the TIL layers in the tubes were collected and counted with a haemocytometer for downstream assays.

5. Peripheral blood mononuclear cell isolation and collection

Human peripheral blood was isolated with heparin (Mochida Pharmaceutical Co., Ltd, Tokyo, Japan)-coated 10mL syringe from the pulmonary artery (PA) of surgically resected primary lung cancer tissues as previously reported [52]. Peripheral blood mononuclear cells were isolated through centrifugation with BD Vacutainer Evacuated Blood Collection Tubes (BD Bioscience) at room temperature in a horizontal rotor for 30 minutes at 1800 RPM according to the manufacturer's instructions. After centrifugation, the blood mononuclear cell layers in the tubes were collected and washed once with 20mL cold PBS containing 1% BSA. Cells were counted with a haemocytometer for downstream assays.

6. T cell purification through magnetic-activated cell labelling and sorting

The immune cells obtained from the tumor tissue or PA blood were resuspended with pre-prepared cold magnetic-activated cell sorting (MACS) buffer (PBS containing 1% BSA and 2mM EDTA). Cells were labelled with anti-CD3 antibody-conjugated microbeads (20 μL per 10^7 total cells; Miltenyi Biotec, Bergisch Gladbach, Germany) for 15 minutes at 4 °C. After centrifugation for 10 minutes at 300 g, the supernatant was aspirated and cell pellets were resuspended in 0.5 mL MACS buffer for subsequent magnetic cell separation.

Magnetic-labelled T cells were positively selected by passing through a medium MACS column in the magnetic field of a MACS Separator. Columns were washed 3 times with MACS buffer, unlabelled cells that pass through were collected for purity check. After removing columns from the separator, the magnetically labelled T cells were flushed out with 1mL added buffer by pushing the plunger into the column. After centrifugation, T cells were resuspended and counted with a haemocytometer for downstream assays. The purity of $CD3^+$ T cells was further confirmed with flow cytometry analysis by checking collected PBMC, unlabelled, and labelled cells.

7. Pan T cell activation and expansion

Culture of T cells constantly requires human recombinant IL-2 (BioLegend, California, United States) to ensure cell viability. Activation and expansion of T cells require further stimulate cells with anti-CD3 and anti-CD28 antibody (BioLegend). Purified T cells were seeded with a density of 1×10^7 cells in 10 mL full RPMI Medium supplemented with IL-2 (600 IU/mL) per well of a 6-well plate. Prepared anti-CD3 and anti-CD28 antibody (20 nM/mL) was added onto the cell suspension. The mixture was incubated at 37 °C in a humidified atmosphere containing 5% CO_2 for 2 days when cell clumps were clearly observed. All antibodys used were listed in Supplementary Table S1.

8. Co-culture system

For the co-culture system of T cells and CAFs (shown in Fig. 5), the Venus-labeled CAFs (2.5×10^5 cells) were plated into each well of 6-well plates. After 24 hours when CAFs have attached to the surface of the petri dish, pre-activated T cells (48 hours stimulation with IL-2, anti-CD3 and anti-CD28 antibody) were added into each well at a density of 7.5×10^5 cells per well. The culture medium was replaced and changed to a 1:1 ratio mixture of CAF culture medium (MEM-α) and T cell culture medium (RPMI1640 with IL-2). After 48 hours of co-culturing, the medium was

collected together with T cells, which later resuspended in FACS buffer or lysed for qRT-PCR analysis. For blocking assay, a CD200R blocking antibody (R&D Systems, Minnesota, United States) was added into the co-culture system together with T cells at the concentration of 50 μg/mL according to the manufacturer's instructions.

For the co-culture system of THP-1 cells and CAFs (shown in Supplementary Fig. S5), the sorted THP-1 cells were stimulated with IL-4 (20 ng/mL; Shenandoah Biotechnology Inc., Pennsylvania, United States) for CD200R expression. Venus-labeled CAFs (2.5×10^5 cells) were seeded into each well of 6-well plates. After 24 hours, IL-4 stimulated THP-1 cells were added into each well at the density of 7.5×10^5 cells per well. The culture medium was replaced and changed to a 1:1 ratio mixture of CAF culture medium (MEM-α) and THP-1 cell culture medium (RPMI1640). After 48 hours of co-culturing, the medium was collected together with THP-1 cells, which later washed once with PBS and then lysed for qRT-PCR analysis. For blocking assay, a CD200 blocking antibody (R&D Systems) was added into the co-culture system together with THP-1 cells at the concentration of 30 μg/mL according to the manufacturer's instructions. All recombinant proteins and antibodies used were shown in Supplementary Table S1.

9. Quantitative real-time reverse transcriptase-polymerase chain reaction (qRT-PCR)

Collected cells were washed once with cold PBS and suspended in 1 ml of TRIzol (Life Technologies) and total RNA was extracted. The cDNA was synthesized using the PrimScript RT reagent Kit with gDNA Eraser (Takara Bio, Shiga, Japan), according to the manufacturer's protocol. RT-PCR was performed in a Thermal Cycler Dice Real-Time System II (TaKaRa) using SYBR Premix Ex Taq II (TaKaRa) and Real-time PCR Primers (hTERT, CDK4R24C, CD200, IFN-y, TNF-a, TGF-β1, IL-4, IL-6, IL-10, IL-12b, VEGFA, CCL2, CSF-1, CXCL12, GAPDH). The sequences of all primers used were shown in Supplemental Table S3.

10. Fluorescence-activated cell sorter (FACS) analysis

The expression of cell surface antigens was determined by using multi-color immunofluorescence staining and a minimum of 10,000 events were counted with FACSDiva software (BD Bioscience). The conjugated antibodies used included the CD3-APC (clone: UCHT1), CD14-APC (clone: 63D3), CD20-APC (clone: 2H7), CD4-APC, CD4-Alexa Fluor 700 (clone: RPA-T4), CD8a-APC, CD8a-Alexa Fluor 700(clone: HIT8a), CD200R-PE, CD200R-APC (clone OX-108), CD279-PE (clone: EH12.2H7), CD152-PE (clone: L3D10), CD366-PE (clone: F38-2E2; BioLegend). The fluorescence-conjugated mouse IgG1 (PE, APC & Alexa Fluor 700; clone: MOPC-21)

and mouse IgG2b (APC; clone: MPC-11) κ isotype Ctrl antibodies (BioLegend) were used as negative controls. Detailed information of all conjugated antibodies used was listed in Supplementary Table S4. In brief, 100-μl of cell suspension (containing 5 × 10^5 cells) were incubated with 5 μl of conjugated antibodies for one hour at 4°C in the dark according to the manufacturer's protocol. Excess antibodies were removed by washing the cells with PBS (containing 3% FBS). FACS analysis was performed by using a FACS Aria II or FACS Accuri C6 plus (BD Bioscience) as indicated in figure legends. Single-spectrum staining of the aforementioned reagents was used for compensation. The final analysis of data was conducted with Flowing Software ver 2.51, which was developed by Perttu Terho (accessed from **http://www.flowingsoftware.com**).

The CD200R-expressing THP-1 and U937 cells were sorted by FACS analysis by using a FACS Aria II (BD Biosciences) after labelled with a fluorescence conjugated CD200R antibody.

Annexin V apoptosis assay was performed with T cells after co-culturing. cells were resuspended in Annexin V Binding Buffer at a concentration of 0. 5 x 10^7 cells/mL, and then stained with 5 μL of APC Annexin V and 10 μL of Propidium Iodide Solution. After 15 min of incubation at room temperature (25°C) in the dark, 400 μL of Annexin V Binding Buffer were added to each tube. The Annexin V

apoptosis assay was analyzed with FACS Accuri C6 plus with proper machine settings according to the manufacturer's instructions.

11. Public database analysis

To explore whether the results could be generalized to a wider population, an analysis was conducted of a TCGA mRNA expression dataset that included 584 primary lung adenocarcinoma patients by using the cBioPortal for Cancer Genomics website (53, 54). Based on the median CD200R1 gene expression, all the samples were divided into 2 groups (the CD200R-high and CD200R-low groups). The correlations between the gene expression of CD200R1 and the gene expression of 6 different immune checkpoints and other 9 immune-related genes were evaluated.

12. Statistical analysis

The significance of differences between any two groups was examined by using Student's t-test (paired or non-paired t-tests as indicated), and $P < 0.05$ was considered as statistically significant unless stated otherwise.

(F.) Acknowledgements

We would like to thank Ms. Hiroko Hashimoto for her technical support. We also would like to show our appreciation to Dr Naoya Sakamoto, Dr Shingo Sakashita, Dr Motohiro Kojima, Dr Satoshi Fujii and Dr Yasushi Uemura for their helpful advice and support.

(G.) References

1. Hanahan D, Coussens LM. Accessories to the crime: functions of cells recruited to the tumor microenvironment. Cancer Cell. 2012 Mar 20;21(3):309-22. doi: 10.1016/j.ccr.2012.02.022.
2. Tlsty TD, Coussens LM. Tumor stroma and regulation of cancer development. Annu Rev Pathol. 2006;1:119-50. doi: 10.1146/annurev.pathol.1.110304.100224.
3. Kalluri R, Zeisberg M. Fibroblasts in cancer. Nat Rev Cancer. 2006 May;6(5):392-401. doi: 10.1038/nrc1877.
4. Kharaishvili G, Simkova D, Bouchalova K, Gachechiladze M, Narsia N, Bouchal J. The role of cancer-associated fibroblasts, solid stress and other microenvironmental factors in tumor progression and therapy resistance. Cancer Cell Int. 2014 May 16;14:41. doi: 10.1186/1475-2867-14-41.
5. Paulsson J, Micke P. Prognostic relevance of cancer-associated fibroblasts in human cancer. Semin Cancer Biol. 2014 Apr;25:61-8. doi: 10.1016/j.semcancer.2014.02.006.
6. Freedman JD, Duffy MR, Lei-Rossmann J, Muntzer A, Scott EM, Hagel J, et al. An oncolytic virus expressing a T-cell engager simultaneously targets cancer and immunosuppressive stromal cells. Cancer Res. 2018 Dec 15;78(24):6852-6865. doi: 10.1158/0008-5472.CAN-18-1750.
7. Mariathasan S, Turley SJ, Nickles D, Castiglioni A, Yuen K, Wang Y, et al. TGFβ

attenuates tumour response to PD-L1 blockade by contributing to exclusion of T cells. Nature. 2018 Feb 22;554(7693):544-548. doi: 10.1038/nature25501.

8. Feig C, Jones JO, Kraman M, Wells RJ, Deonarine A, Chan DS, et al. Targeting CXCL12 from FAP-expressing carcinoma-associated fibroblasts synergizes with anti-PD-L1 immunotherapy in pancreatic cancer. Proc Natl Acad Sci U S A. 2013 Dec 10;110(50):20212-7. doi: 10.1073/pnas.1320318110.
9. Costa A, Kieffer Y, Scholer-Dahirel A, Pelon F, Bourachot B, Cardon M, et al. Fibroblast heterogeneity and immunosuppressive environment in human breast cancer. Cancer Cell. 2018 Mar 12;33(3):463-479.e10. doi: 10.1016/j.ccell.2018.01.011.
10. Kieffer Y, Hocine HR, Gentric G, Pelon F, Bernard C, Bourachot B, et al. Single-cell analysis reveals fibroblast clusters linked to immunotherapy resistance in cancer. Cancer Discov. 2020 Sep;10(9):1330-1351. doi: 10.1158/2159-8290.CD-19-1384.
11. Lakins MA, Ghorani E, Munir H, Martins CP, Shields JD. Cancer-associated fibroblasts induce antigen-specific deletion of CD8 + T Cells to protect tumour cells. Nat Commun. 2018 Mar 5;9(1):948. doi: 10.1038/s41467-018-03347-0.
12. Rittmeyer A, Barlesi F, Waterkamp D, Park K, Ciardiello F, von Pawel J, et al. Atezolizumab versus docetaxel in patients with previously treated non-small-cell lung cancer (OAK): a phase 3, open-label, multicentre randomised controlled trial. Lancet. 2017 Jan 21;389(10066):255-265. doi: 10.1016/S0140-6736(16)32517-X.

13. Herbst RS, Baas P, Kim DW, Felip E, Pérez-Gracia JL, Han JY, et al. Pembrolizumab versus docetaxel for previously treated, PD-L1-positive, advanced non-small-cell lung cancer (KEYNOTE-010): a randomised controlled trial. Lancet. 2016 Apr 9;387(10027):1540-1550. doi: 10.1016/S0140-6736(15)01281-7.

14. Rijkers ES, de Ruiter T, Baridi A, Veninga H, Hoek RM, Meyaard L. The inhibitory CD200R is differentially expressed on human and mouse T and B lymphocytes. Mol Immunol. 2008 Feb;45(4):1126-35. doi: 10.1016/j.molimm.2007.07.013.

15. Najar M, Raicevic G, Jebbawi F, De Bruyn C, Meuleman N, Bron D, et al. Characterization and functionality of the CD200-CD200R system during mesenchymal stromal cell interactions with T-lymphocytes. Immunol Lett. 2012 Aug 30;146(1-2):50-6. doi: 10.1016/j.imlet.2012.04.017.

16. Jenmalm MC, Cherwinski H, Bowman EP, Phillips JH, Sedgwick JD. Regulation of myeloid cell function through the CD200 receptor. J Immunol. 2006 Jan 1;176(1):191-9. doi: 10.4049/jimmunol.176.1.191.

17. Gorczynski R, Chen Z, Kai Y, Lee L, Wong S, Marsden PA. CD200 is a ligand for all members of the CD200R family of immunoregulatory molecules. J Immunol. 2004 Jun 15;172(12):7744-9. doi: 10.4049/jimmunol.172.12.7744.

18. Zhang S, Cherwinski H, Sedgwick JD, Phillips JH. Molecular mechanisms of CD200 inhibition of mast cell activation. J Immunol. 2004 Dec 1;173(11):6786-93. doi:

10.4049/jimmunol.173.11.6786.

19. Prodeus A, Cydzik M, Abdul-Wahid A, Huang E, Khatri I, Gorczynski R, et al. Agonistic CD200R1 DNA aptamers are potent immunosuppressants that prolong allogeneic skin graft survival. Mol Ther Nucleic Acids. 2014 Aug 26;3(8):e190. doi: 10.1038/mtna.2014.41.

20. Gorczynski RM, Chen Z, Lee L, Yu K, Hu J. Anti-CD200R ameliorates collagen-induced arthritis in mice. Clin Immunol. 2002 Sep;104(3):256-64. doi: 10.1006/clim.2002.5232. PMID: 12217336.

21. Prodeus A, Sparkes A, Fischer NW, Cydzik M, Huang E, Khatri I, et al. A synthetic cross-species CD200R1 agonist suppresses inflammatory immune responses in vivo. Mol Ther Nucleic Acids. 2018 Sep 7;12:350-358. doi: 10.1016/j.omtn.2018.05.023.

22. Liu JQ, Talebian F, Wu L, Liu Z, Li MS, Wu L, et al. A critical role for CD200R signaling in limiting the growth and metastasis of CD200+ melanoma. J Immunol. 2016 Aug 15;197(4):1489-97. doi: 10.4049/jimmunol.1600052.

23. Erin N, Podnos A, Tanriover G, Duymuş Ö, Cote E, Khatri I, et al. Bidirectional effect of CD200 on breast cancer development and metastasis, with ultimate outcome determined by tumor aggressiveness and a cancer-induced inflammatory response. Oncogene. 2015 Jul;34(29):3860-70. doi: 10.1038/onc.2014.317

24. Huang S, Pan Y, Zhang Q, Sun W. Role of CD200/CD200R signaling pathway in

regulation of CD4+T cell subsets during thermal ablation of hepatocellular carcinoma. Med Sci Monit. 2019 Mar 6;25:1718-1728. doi: 10.12659/MSM.913094.

25. Zhang SS, Huang ZW, Li LX, Fu JJ, Xiao B. Identification of CD200+ colorectal cancer stem cells and their gene expression profile. Oncol Rep. 2016 Oct;36(4):2252-60. doi: 10.3892/or.2016.5039.
26. Yoshimura K, Suzuki Y, Inoue Y, Tsuchiya K, Karayama M, Iwashita Y, et al. CD200 and CD200R1 are differentially expressed and have differential prognostic roles in non-small cell lung cancer. Oncoimmunology. 2020 Apr 7;9(1):1746554. doi: 10.1080/2162402X.2020.1746554.
27. Blom LH, Martel BC, Larsen LF, Hansen CV, Christensen MP, Juel-Berg N, et al. The immunoglobulin superfamily member CD200R identifies cells involved in type 2 immune responses. Allergy. 2017 Jul;72(7):1081-1090. doi: 10.1111/all.13129.
28. Ishibashi M, Neri S, Hashimoto H, Miyashita T, Yoshida T, Nakamura Y, et al. CD200-positive cancer associated fibroblasts augment the sensitivity of Epidermal Growth Factor Receptor mutation-positive lung adenocarcinomas to EGFR Tyrosine kinase inhibitors. Sci Rep. 2017 Apr 21;7:46662. doi: 10.1038/srep46662.
29. Hoek RM, Ruuls SR, Murphy CA, Wright GJ, Goddard R, Zurawski SM, et al. Down-regulation of the macrophage lineage through interaction with OX2 (CD200). Science. 2000 Dec 1;290(5497):1768-71. doi: 10.1126/science.290.5497.1768.

30. Wright GJ, Jones M, Puklavec MJ, Brown MH, Barclay AN. The unusual distribution of the neuronal/lymphoid cell surface CD200 (OX2) glycoprotein is conserved in humans. Immunology. 2001 Feb;102(2):173-9. doi: 10.1046/j.1365-2567.2001.01163.x.

31. Wright GJ, Cherwinski H, Foster-Cuevas M, Brooke G, Puklavec MJ, Bigler M, et al. Characterization of the CD200 receptor family in mice and humans and their interactions with CD200. J Immunol. 2003 Sep 15;171(6):3034-46. doi: 10.4049/jimmunol.171.6.3034.

32. Hashimoto H, Suda Y, Miyashita T, Ochiai A, Tsuboi M, Masutomi K, et al. A novel method to generate single-cell-derived cancer-associated fibroblast clones. J Cancer Res Clin Oncol. 2017 Aug;143(8):1409-1419. doi: 10.1007/s00432-017-2409-3.

33. Neri S, Hashimoto H, Kii H, Watanabe H, Masutomi K, Kuwata T, et al. Cancer cell invasion driven by extracellular matrix remodeling is dependent on the properties of cancer-associated fibroblasts. J Cancer Res Clin Oncol. 2016 Feb;142(2):437-46. doi: 10.1007/s00432-015-2046-7.

34. Chen DS, Mellman I. Oncology meets immunology: the cancer-immunity cycle. Immunity. 2013 Jul 25;39(1):1-10. doi: 10.1016/j.immuni.2013.07.012.

35. Kataki A, Scheid P, Piet M, Marie B, Martinet N, Martinet Y, et al. Tumor infiltrating lymphocytes and macrophages have a potential dual role in lung cancer by supporting both host-defense and tumor progression. J Lab Clin Med. 2002 Nov;140(5):320-8. doi:

10.1067/mlc.2002.128317.

36. Jin HT, Anderson AC, Tan WG, West EE, Ha SJ, Araki K, et al. Cooperation of Tim-3 and PD-1 in CD8 T-cell exhaustion during chronic viral infection. Proc Natl Acad Sci U S A. 2010 Aug 17;107(33):14733-8. doi: 10.1073/pnas.1009731107.

37. Blackburn SD, Shin H, Haining WN, Zou T, Workman CJ, Polley A, et al. Coregulation of CD8+ T cell exhaustion by multiple inhibitory receptors during chronic viral infection. Nat Immunol. 2009 Jan;10(1):29-37. doi: 10.1038/ni.1679.

38. Joller N, Hafler JP, Brynedal B, Kassam N, Spoerl S, Levin SD, et al. Cutting edge: TIGIT has T cell-intrinsic inhibitory functions. J Immunol. 2011 Feb 1;186(3):1338-42. doi: 10.4049/jimmunol.1003081.

39. Barber DL, Wherry EJ, Masopust D, Zhu B, Allison JP, Sharpe AH, et al. Restoring function in exhausted CD8 T cells during chronic viral infection. Nature. 2006 Feb 9;439(7077):682-7. doi: 10.1038/nature04444.

40. Paley MA, Kroy DC, Odorizzi PM, Johnnidis JB, Dolfi DV, Barnett BE, et al. Progenitor and terminal subsets of CD8+ T cells cooperate to contain chronic viral infection. Science. 2012 Nov 30;338(6111):1220-5. doi: 10.1126/science.1229620.

41. Im SJ, Hashimoto M, Gerner MY, Lee J, Kissick HT, Burger MC, et al. Defining CD8+ T cells that provide the proliferative burst after PD-1 therapy. Nature. 2016 Sep 15;537(7620):417-421. doi: 10.1038/nature19330.

42. Miller BC, Sen DR, Al Abosy R, Bi K, Virkud YV, LaFleur MW, et al. Subsets of exhausted CD8+ T cells differentially mediate tumor control and respond to checkpoint blockade. Nat Immunol. 2019 Mar;20(3):326-336. doi: 10.1038/s41590-019-0312-6.

43. Thommen DS, Koelzer VH, Herzig P, Roller A, Trefny M, Dimeloe S, et al. A transcriptionally and functionally distinct PD-1+ CD8+ T cell pool with predictive potential in non-small-cell lung cancer treated with PD-1 blockade. Nat Med. 2018 Jul;24(7):994-1004. doi: 10.1038/s41591-018-0057-z.

44. Odorizzi PM, Pauken KE, Paley MA, Sharpe A, Wherry EJ. Genetic absence of PD-1 promotes accumulation of terminally differentiated exhausted CD8+ T cells. J Exp Med. 2015 Jun 29;212(7):1125-37. doi: 10.1084/jem.20142237.

45. Caserta S, Nausch N, Sawtell A, Drummond R, Barr T, Macdonald AS, et al. Chronic infection drives expression of the inhibitory receptor CD200R, and its ligand CD200, by mouse and human CD4 T cells. PLoS One. 2012;7(4):e35466. doi: 10.1371/journal.pone.0035466.

46. J Duraiswamy J, Kaluza KM, Freeman GJ, Coukos G. Dual blockade of PD-1 and CTLA-4 combined with tumor vaccine effectively restores T-cell rejection function in tumors. Cancer Res. 2013 Jun 15;73(12):3591-603. doi: 10.1158/0008-5472.CAN-12-4100.

47. Wei SC, Anang NAS, Sharma R, Andrews MC, Reuben A, Levine JH, et al. Combination

anti-CTLA-4 plus anti-PD-1 checkpoint blockade utilizes cellular mechanisms partially distinct from monotherapies. Proc Natl Acad Sci U S A. 2019 Nov 5;116(45):22699-22709. doi: 10.1073/pnas.1821218116.

48. Huang RY, Francois A, McGray AR, Miliotto A, Odunsi K. Compensatory upregulation of PD-1, LAG-3, and CTLA-4 limits the efficacy of single-agent checkpoint blockade in metastatic ovarian cancer. Oncoimmunology. 2016 Oct 28;6(1):e1249561. doi: 10.1080/2162402X.2016.1249561.

49. Gao J, Navai N, Alhalabi O, Siefker-Radtke A, Campbell MT, Tidwell RS, et al. Neoadjuvant PD-L1 plus CTLA-4 blockade in patients with cisplatin-ineligible operable high-risk urothelial carcinoma. Nat Med. 2020 Oct 12. doi: 10.1038/s41591-020-1086-y. Epub ahead of print.

50. Mahadevan D, Lanasa MC, Farber C, Pandey M, Whelden M, Faas SJ, et al. Phase I study of samalizumab in chronic lymphocytic leukemia and multiple myeloma: blockade of the immune checkpoint CD200. J Immunother Cancer. 2019 Aug 23;7(1):227. doi: 10.1186/s40425-019-0710-1.

51. Lambrechts D, Wauters E, Boeckx B, Aibar S, Nittner D, Burton O, et al. Phenotype molding of stromal cells in the lung tumor microenvironment. Nat Med. 2018 Aug;24(8):1277-1289. doi: 10.1038/s41591-018-0096-5.

52. Maeda R, Ishii G, Neri S, Aoyagi K, Haga H, Sasaki H, et al. Circulating CD14+CD204+

cells predict postoperative recurrence in non-small-cell lung cancer patients. J Thorac Oncol. 2014 Feb;9(2):179-88. doi: 10.1097/JTO.0000000000000044.

53. Cerami E, Gao J, Dogrusoz U, Gross BE, Sumer SO, Aksoy BA, et al. The cBio cancer genomics portal: an open platform for exploring multidimensional cancer genomics data. Cancer Discov. 2012 May;2(5):401-4. doi: 10.1158/2159-8290.CD-12-0095.

54. Gao J, Aksoy BA, Dogrusoz U, Dresdner G, Gross B, Sumer SO, et al. Integrative analysis of complex cancer genomics and clinical profiles using the cBioPortal. Sci Signal. 2013 Apr 2;6(269):pl1. doi: 10.1126/scisignal.2004088.

(H.) Figure Legends

Table. 1. *Pathological characteristics of CD200-expressing CAFs within 19 cases.*

Fig. 1. *Investigation of CD200 expression within CAF library.*

(A.) CD200 mRNA expression among 19 CAF samples by RT-PCR.

(B.) CD200 protein expression among 19 CAF samples analyzed with FACS Accuri.

Fig. 2. *Life extension and construction of CD200 overexpress and shRNA knockdown CAF cell lines.*

(A.) The mRNA expression of hTERT and CDK4 within selected CAF samples by RT-PCR.

(B.) CD200 protein expression within CD200 shRNA knockdown CAF sample analyzed with FACS Accuri.

(C.) CD200 protein expression within CD200 overexpress CAF sample analyzed with FACS Accuri.

Fig. 3. *CD200R expressing cells within tumor-infiltrating leukocytes (TILs)*

(A.) Gating strategy for lymphocytes (R-1) and monocytes (R-2), and selecting for single

cells (R-4).

(B.) FACS analysis (FACS Aria) of CD200R+ cells in CD3 (left), CD14 (middle) and CD20 (right) cells.

(C.) The proportion of CD3+ T cells, CD14+ monocytes and CD20+ B cells within extracted TILs.

N=10, Asterisk, $P < 0.05$ according to Student's t-test.

(D.) The proportion of CD200R+ cells within each cell populations.

N=10, Asterisk, $P < 0.05$ according to Student's t-test.

Fig. 4. *CD200R expressing cells within peripheral blood mononuclear cells (PBMCs) extracted from pulmonary artery (PA) blood analyzed with FACS Aria.*

(A.) Gating strategy of PBMCs extracted from PA blood.

(B.) FACS analysis of CD3+ T cells (left), CD14+ monocytes (middle) and CD20+ B cells (right) in PA blood from one NSCLC sample.

(C.) Purity analysis of MACS-sorted CD3+ T cells extracted from PA blood.

(D.) The proportion of T cells with CD200R+/CD3+, CD200R+/CD4+ or CD200R+/CD8+ among all CD3+ T cells extracted from PA blood.

N=12, Asterisk, $P < 0.05$ according to Student's t-test.

(E.) The proportion of CD200R+ cells within the CD4 and CD8 T cell populations.

N=12, Asterisk, $P < 0.05$ according to Student's t-test.

Fig. 5. *Scheme of co-culture system for CD200-CD200R axis interaction between CAFs and T cells.*

Fig. 6. *Investigate cytokine expression pattern and functional assay for checking CD200-CD200R axis interaction between CAFs and T cells.*

(A.) The mRNA expression level of multiple cytokines was checked with RT-PCR among two T cell samples.

(B.) T cell apoptosis and necrosis level were checked with Annexin V and PI by FACS analysis (FACS Accuri).

Fig. 7. *Investigate cell-cell interaction and CD200-CD200R interaction between CAFs and T cells.*

(A.) The mRNA expression level of multiple cytokines was checked with RT-PCR among two T cell samples with different concentration of recombinant CD200.

(B.) The mRNA expression level of IL-4 was checked with RT-PCR among two T cell samples co-cultured with CAFs with a CD200R blocking antibody.

Fig. 8. *Comparison of the proportions of CD200R+ T cells in PA blood and TILs analyzed with FACS Aria.*

(A.) The proportion of CD200R+ T cells in CD3+ cells from the PA and TIL (non-paired) samples.

N=12, Asterisk, $P < 0.05$ according to non-paired Student's t-test.

(B.) The proportion of CD200R+ T cells in CD3+ cells from the PA and TIL (paired) samples.

N=3; analyzed with paired Student's t-test.

Fig. 9. *Co-expression of other immune checkpoints in T cells analyzed with FACS Aria.*

(A.) The proportion of T cells co-expressing CD200R and the immune checkpoint PD-1 within CD3+ (left), CD4+ and CD8+ T cells (right) from the paired PA and TIL samples.

N=3; conducted with Student's t-test.

(B.) The proportion of T cells co-expressing CD200R and the immune checkpoint CTLA-4 within CD3+ (left), CD4+ and CD8+ T cells (right) from the paired PA and TIL samples.

N=3; analyzed with Student's t-test.

(C.) The proportion of T cells co-expressing CD200R and the immune checkpoint TIM-3 within CD3+ (left), CD4+ and CD8+ T cells (right) from the paired PA and TIL samples

N=3; analyzed with Student's t-test.

Fig. 10 and Fig. 11. *The expression of CD200R in lung adenocarcinoma and its correlation with immune checkpoints according to public database analysis.*

Comparing the co-expression of mRNA between samples, separated according to medium expression valve (CD200R-low and CD200R-high group). Cohort: lung adenocarcinoma (TCGA, Source data from GDAC Firehose), 517 samples derived from 516 patients. (PDCD1: PD-1; HAVCR2: TIM-3; LAG-3, CTLA-4, TIGIT, IDO1).

Supplementary Fig. S1.

(A.) Surface protein expression of CD200 within CAF 608 analyzed with FACS Accuri.

(B.) Surface protein expression of CD200 within CAF 721pm analyzed with FACS Accuri.

(C.) Surface protein expression of CD200 within CAF 1228 analyzed with FACS Accuri.

Supplementary Fig. S2.

(A.) Lentivirus-mediated gene transfer of hTERT and CDK4R24C.

(D.) Surface protein expression of CD200 within CD200 shRNA knockdown CAF sample analyzed with FACS Accuri.

Supplementary Fig. S3.

Negative controls for lymphocytes (R-1) and monocytes (R-2) analyzed with FACS Aria.

Supplementary Fig. S4.

(A.) Purity analysis (FACS Aria) for magnetic-activated cell sorting (MACS) sorted-CD3- cells in PA blood (left and middle), and negative control for CD3+ cells in PA (right).

(B.) Purity analysis of MACS-sorted CD3+ T cells in TILs.

(C.) Negative control (left) and purity analysis (right) of MACS-sorted CD3- cells in TILs.

(D.) Gating strategy for CD4+ and CD8+ T cells in MACS-sorted CD3+ cells from PA.

Supplementary Fig. S5.

(A.) Establishing CD200R expressing THP-1 cell lines through FACS cell sorting and IL-4 stimulation analyzed with FACS Accuri.

(B.) Establishing CD200R expressing U937 cell lines through FACS cell sorting and IL-4 stimulation analyzed with FACS Accuri.

(C.) Establishing CD200R shRNA knockdown THP-1 cell lines through lentivirus-mediated gene transfer and IL-4 stimulation analyzed with FACS Accuri.

(D.) Scheme of co-culture experiment for CD200-CD200R axis interaction between CAFs and THP-1 cells.

Supplementary Fig. S6.

(A.) The mRNA expression level of multiple cytokines was checked with RT-PCR with two T cell samples separately.

(B.) The mRNA expression level of multiple cytokines was checked with RT-PCR with THP-1 cells co-cultured with CAFs.

(C.) The mRNA expression level of IL-6 was checked with RT-PCR with THP-1 and U937 cell lines co-cultured with CAFs.

Supplementary Fig. S7.

(A.) The mRNA expression level of multiple cytokines was checked with RT-PCR with two T cell samples with different concentration of recombinant CD200 separately.

(B.) The mRNA expression level of IL-6 was checked with RT-PCR among THP-1 cell

lines co-cultured with CAFs.

Supplementary Fig. S8.

(A.) The proportion of CD200R among CD4+ T cells between paired PA and TIL samples analyzed with FACS Aria.

N=3; analyzed with Student's t-test.

(B.) The proportion of CD200R in CD8+ T cells in the paired PA and TIL samples analyzed with FACS Aria.

N=3; analyzed with Student's t-test.

Supplementary Fig. S9.

(A.) FACS analysis (FACS Aria) of the co-expression of CD200R with the immune checkpoints PD-1 (left), CTLA-4 (middle) and TIM-3 (right) within the CD3+ T cell populations from the PA blood of one NSCLC sample.

(B.) FACS analysis (FACS Aria) of the co-expression of CD200R with the immune checkpoint PD-1 （left）, CTLA-4 (middle) and TIM-3 (right) within the CD3+ T cell populations from TIL of the same NSCLC sample.

(C.) FACS analysis (FACS Aria) of the co-expression of CD200R with the immune checkpoint PD-1 within the CD4+ or CD8+ T cell populations from the PA blood of

the same NSCLC sample.

(D.) FACS analysis (FACS Aria) of the co-expression of CD200R with the immune checkpoint PD-1 within the CD4+ or CD8+ T cell populations from the TILs of the same NSCLC sample.

Supplementary Fig. S10.

Comparing the co-expression of mRNA between samples, separated according to medium expression valve (CD200R-low and CD200R-high group). Cohort: lung adenocarcinoma (TCGA, Firehose Legacy), 517 samples derived from 516 patients. (IRF4; ICOS; GATA3; CD274: PD-L1; STAT4, CXCR5, FOXP3, STK11, PRKCI).

Supplementary Fig. S11.

(A.) Correlation of CD200 and CD200R mRNA expression.

(B.) Overall survival and Disease-free survival between CD200 high and low expression groups.

(C.) Overall survival and Disease-free survival between CD200R high and low expression groups.

Supplementary Fig. S12. *Plasmid used within lentivirus-mediated gene transfer.*

Supplementary Table S1. *List of antibodies used in T cell culture or Functional assays.*

Supplementary Table S2. *The shRNA sequence used in gene knockdown.*

Supplementary Table S3. *List of primers used in rt-PCR.*

Supplementary Table S4. *List of antibodies used in Flow cytometry analysis.*

Table 1.

Characteristics		No. of patients (%)	CD200-positive CAFs		P value† Chi-square test
		No. of patients (%)	Absent	Present	
Total		19	15 (79)	4 (21)	
Age	< 65	6 (32)	1 (25)	5 (33)	1.000
	≥ 65	13 (68)	3 (75)	10 (67)	
Gender	Female	7 (37)	1 (25)	6 (40)	1.000
	Male	12(63)	3 (75)	9 (60)	
Smoking	Absent	6 (32)	1 (25)	5 (33)	1.000
	Present	13 (68)	3 (75)	10 (67)	
Tumor size (cm)	≤ 3.0	7 (37)	0 (0)	7 (47)	0.245
	> 3.0	12(63)	4 (100)	8 (53)	
Lymph node metastasis	Absent	10 (53)	1 (25)	9 (60)	0.303
	Present	9 (47)	3 (75)	6 (40)	
Local invasion	Absent	8 (42)	1 (25)	7 (47)	0.603
	Present	11 (58)	3 (75)	8 (53)	

Figure 1.

A.

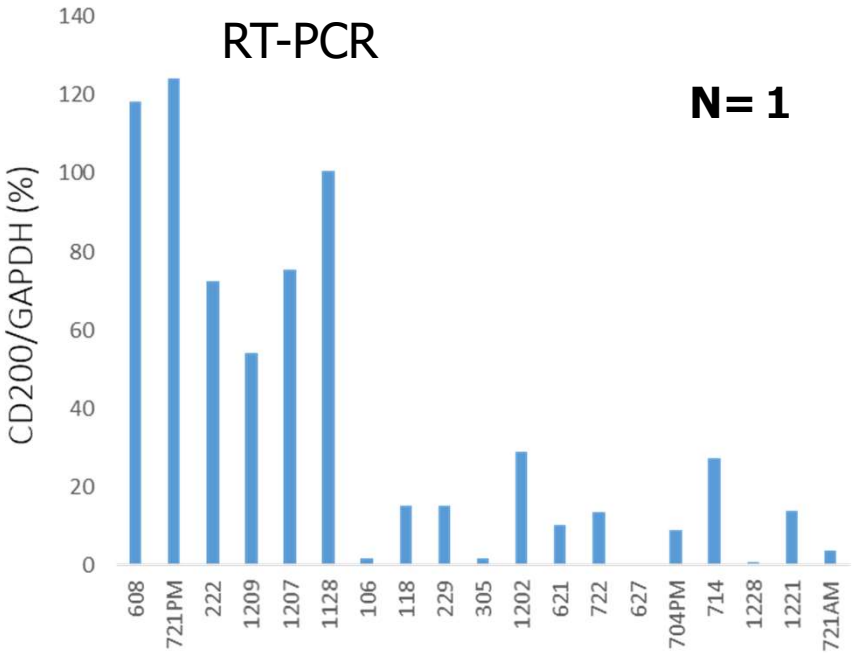
RT-PCR
N= 1
CD200/GAPDH (%)
140
120
100
80
60
40
20
0
608
721PM
222
1209
1207
1128
106
118
229
305
1202
621
722
627
704PM
714
1228
1221
721AM

B.

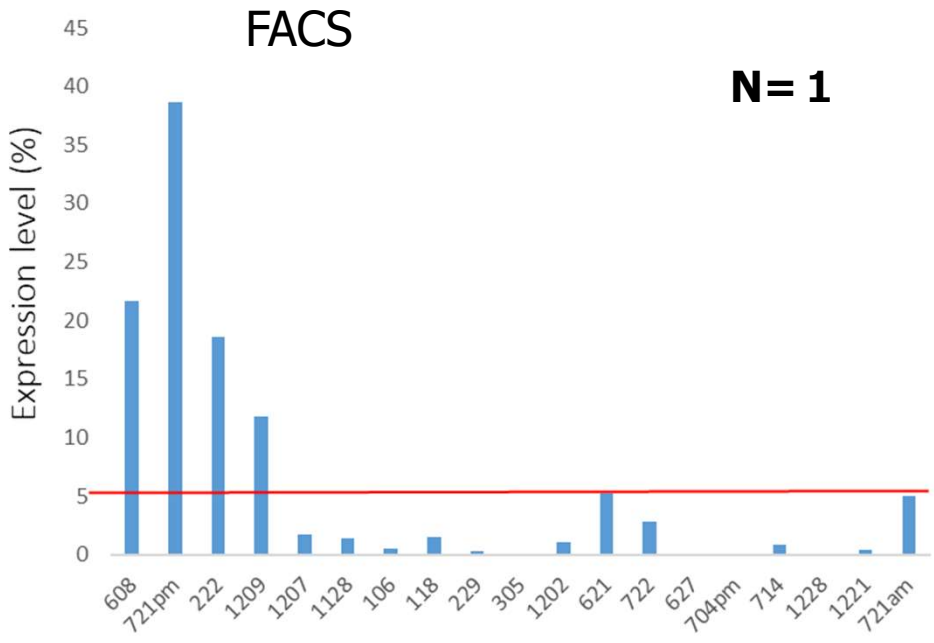
FACS
N= 1
Expression level (%)
45
40
35
30
25
20
15
10
5
0
608
721pm
222
1209
1207
1128
106
118
229
305
1202
621
722
627
704pm
714
1228
1221
721am

Figure 2.

A.

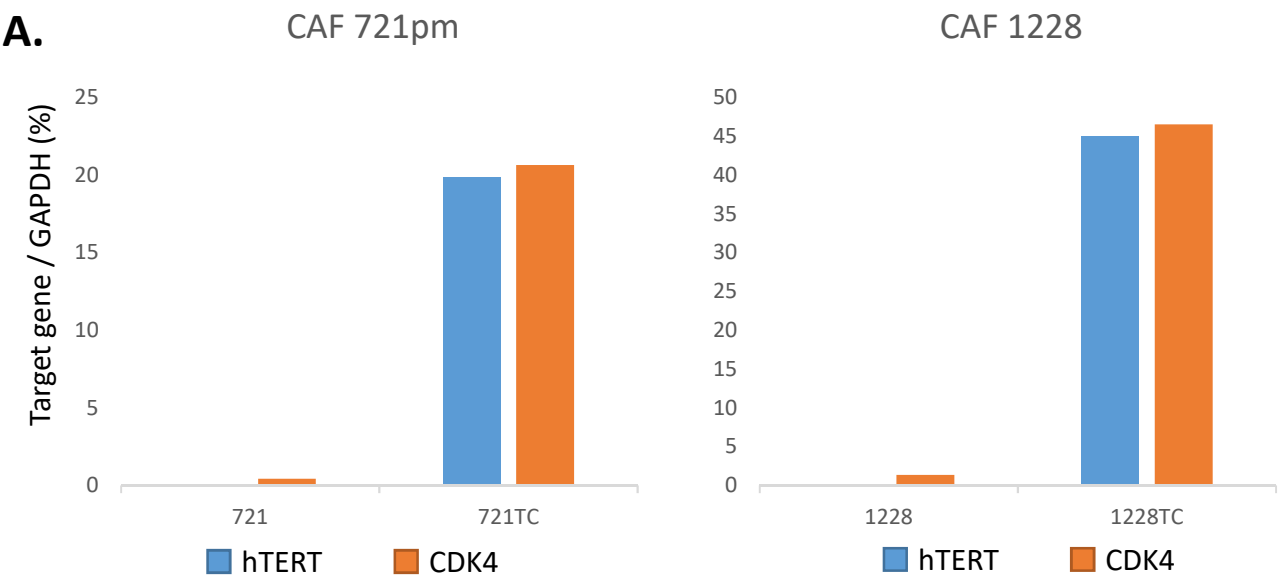

B.

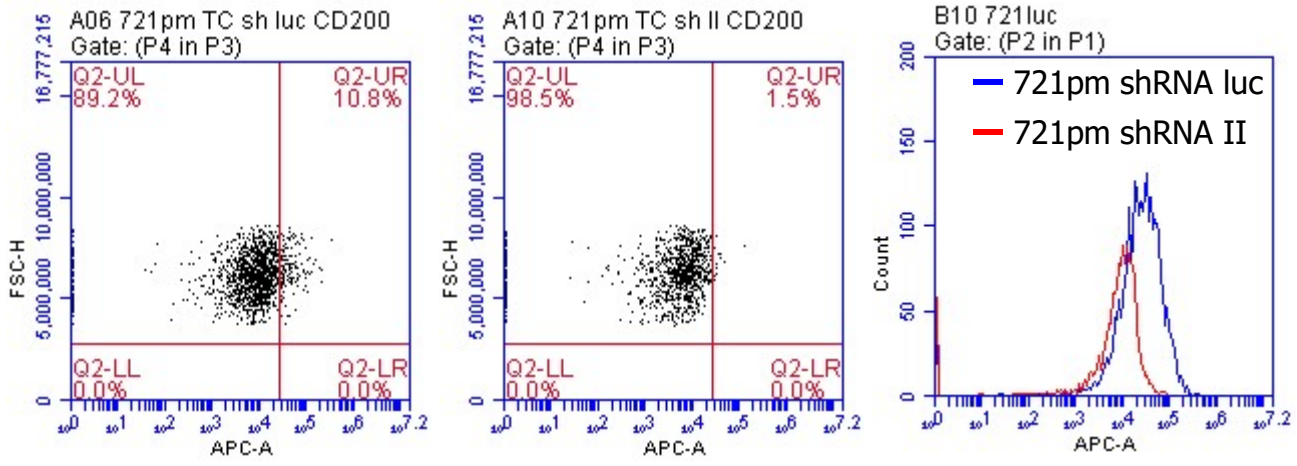

shRNA luc (con) shRNA No.2

C.

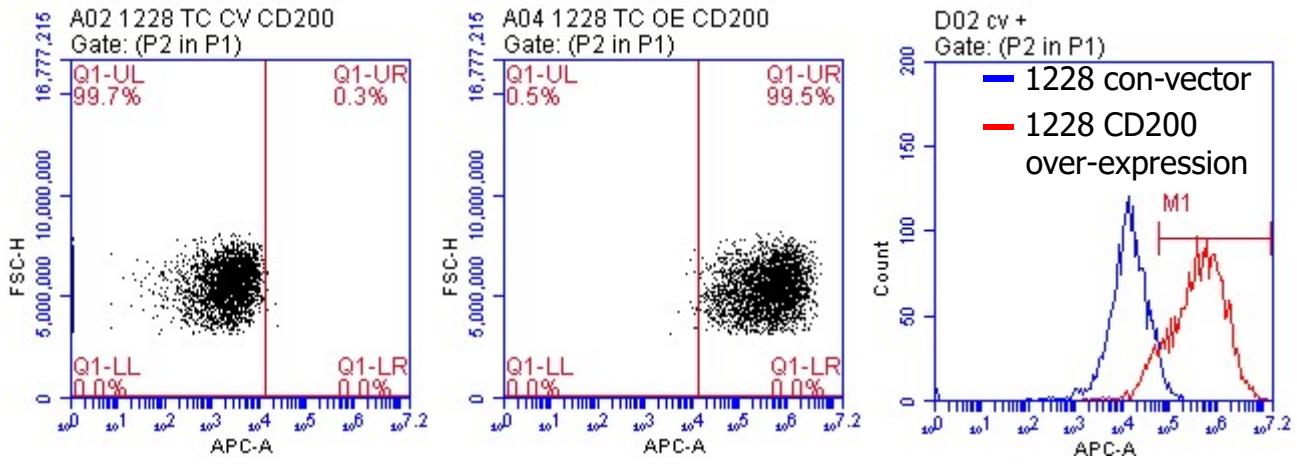

Control Vector CD200 overexpression

Figure 3.

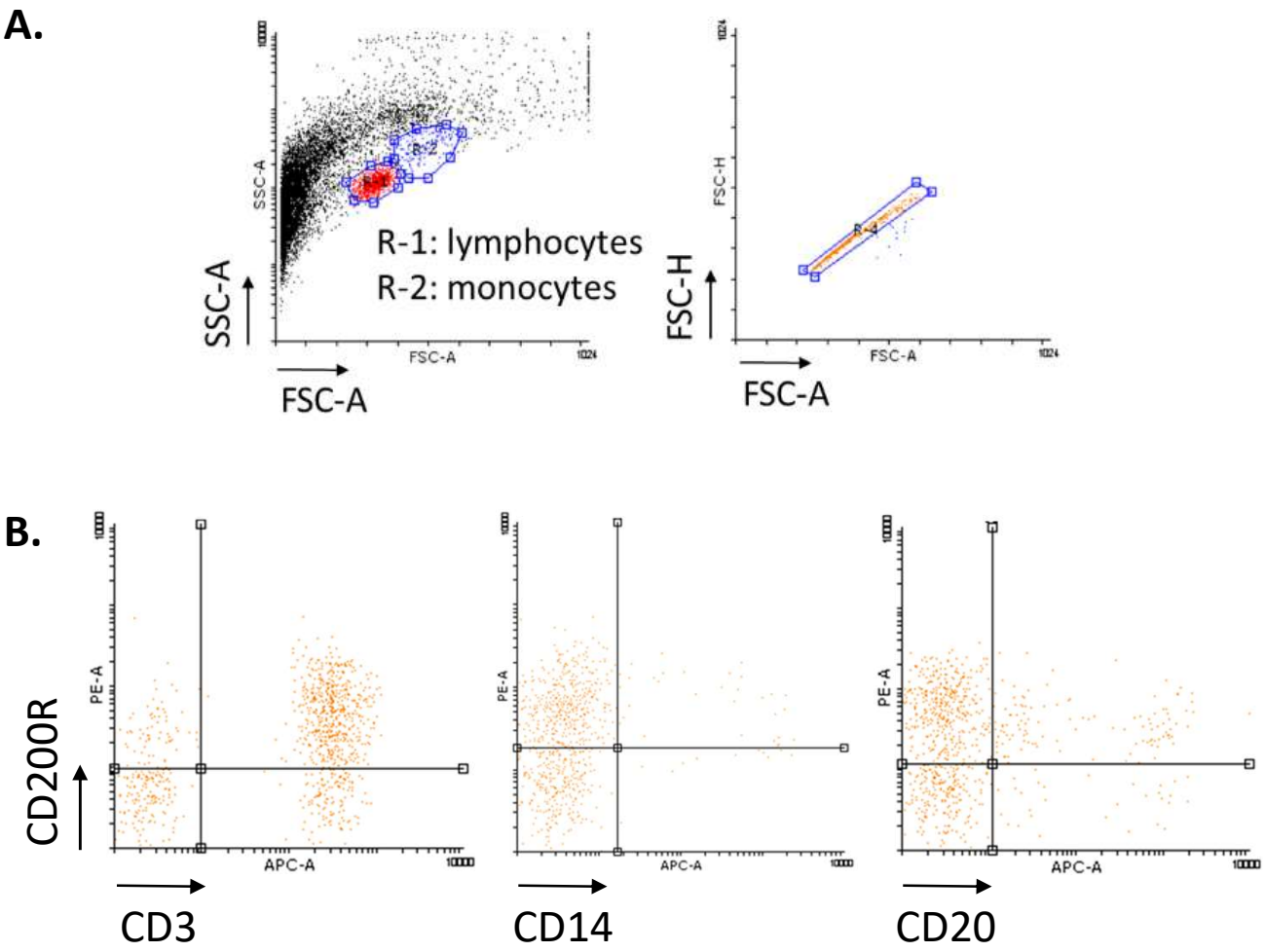
A.
SSC-A
FSC-A
R-1: lymphocytes
R-2: monocytes
FSC-H
FSC-A
B.
CD200R
PE-A
APC-A
CD3
CD14
CD20
C.
Cell number/ total tumour-infiltrating leukocytes (%)
N=10
CD3
CD14
CD20
D.
CD200R+ cells (%)
N=10
CD3
CD14
CD20

Figure 4.

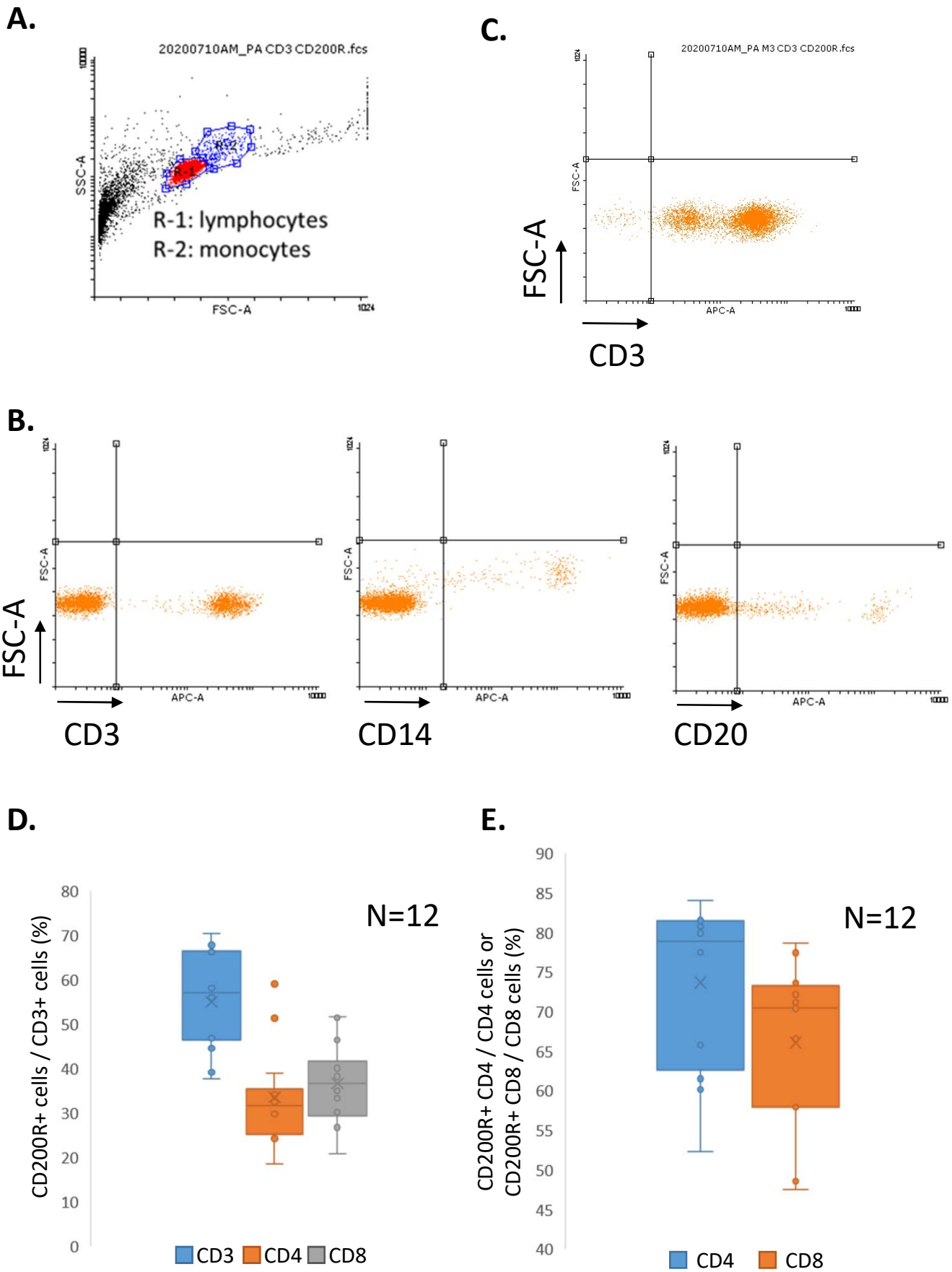
A.
20200710AM_PA CD3 CD200R.fcs
SSC-A
FSC-A
R-1: lymphocytes
R-2: monocytes
C.
20200710AM_PA M3 CD3 CD200R.fcs
FSC-A
APC-A
FSC-A
CD3
B.
FSC-A
APC-A
CD3
CD14
CD20
D.
CD200R+ cells / CD3+ cells (%)
N=12
CD3
CD4
CD8
E.
CD200R+ CD4 / CD4 cells or CD200R+ CD8 / CD8 cells (%)
N=12
CD4
CD8

Figure 5.

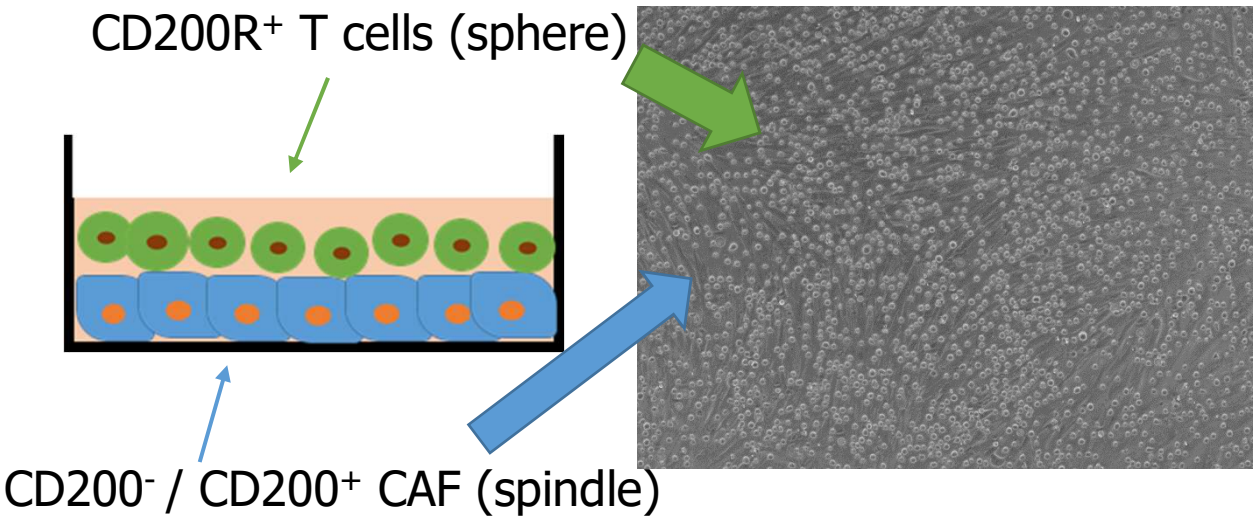
CD200R+ T cells (sphere)
CD200- / CD200+ CAF (spindle)

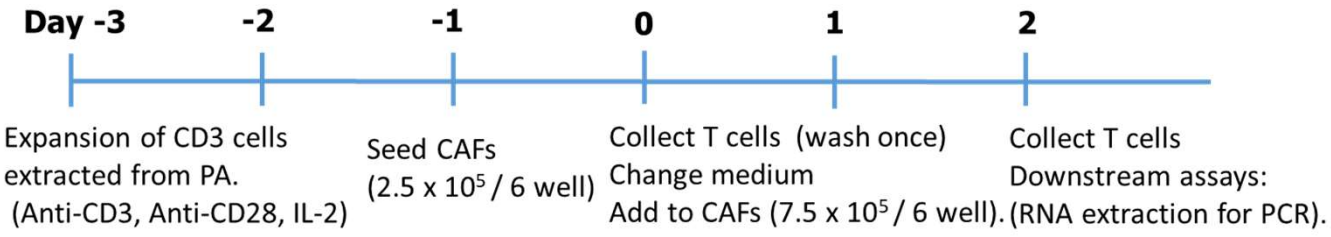
Day -3
-2
-1
0
1
2
Expansion of CD3 cells extracted from PA. (Anti-CD3, Anti-CD28, IL-2)
Seed CAFs (2.5 x 10^5 / 6 well)
Collect T cells (wash once) Change medium Add to CAFs (7.5 x 10^5 / 6 well).
Collect T cells Downstream assays: (RNA extraction for PCR).

Figure 6.

A. Cytokines (RT-PCR)

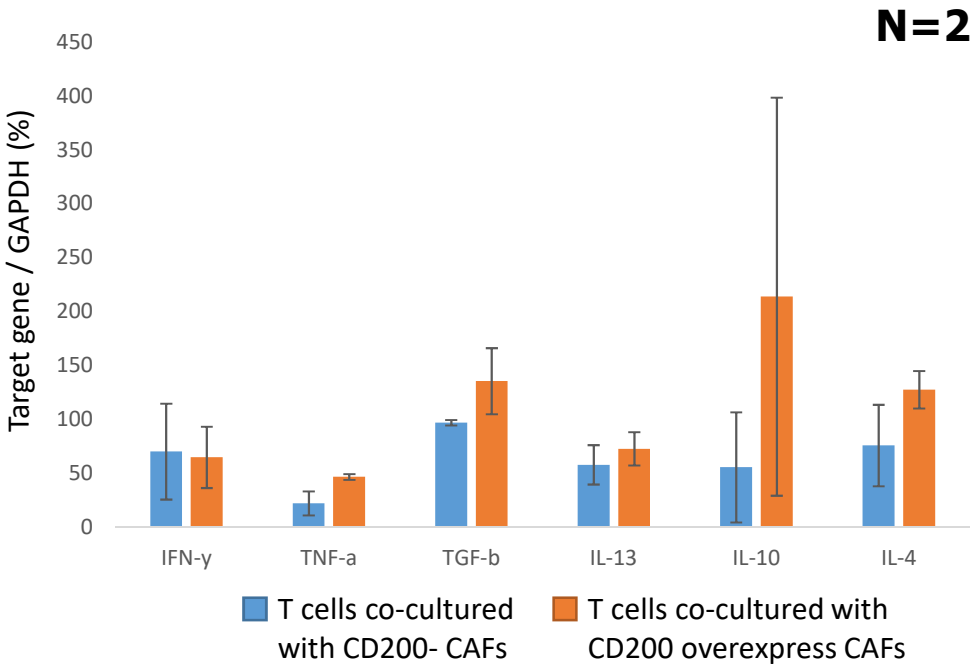

B. Apoptosis (FACS)

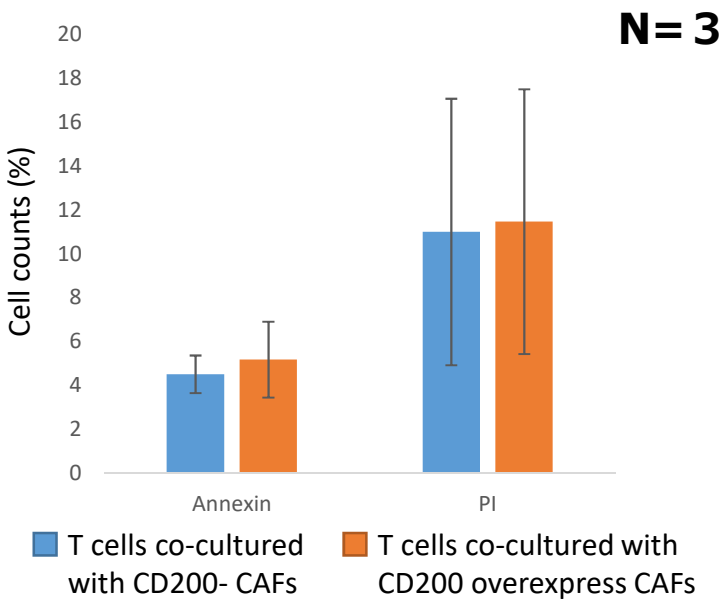

Figure 7.

A. Cytokines (RT-PCR)

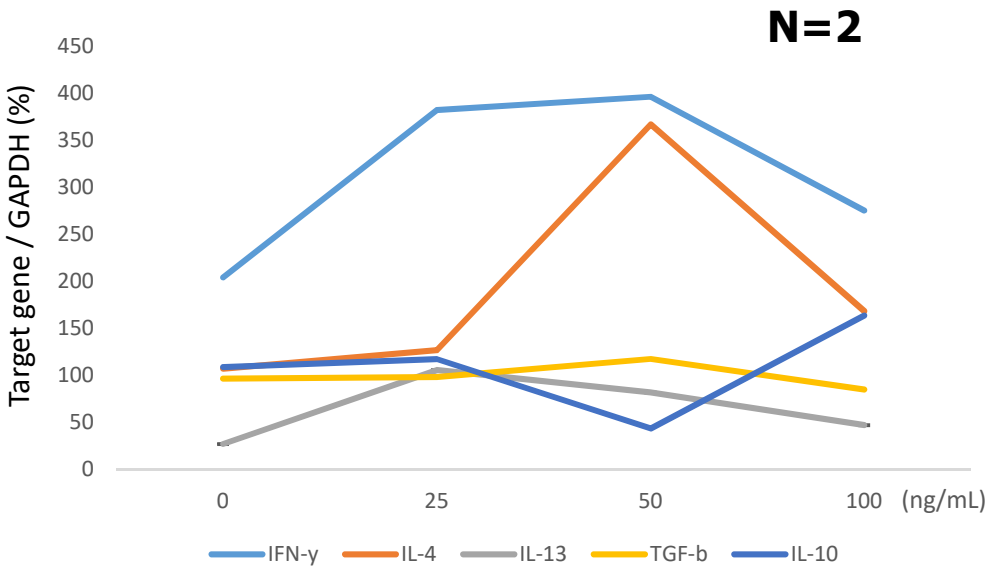

B. IL-4 (RT-PCR)

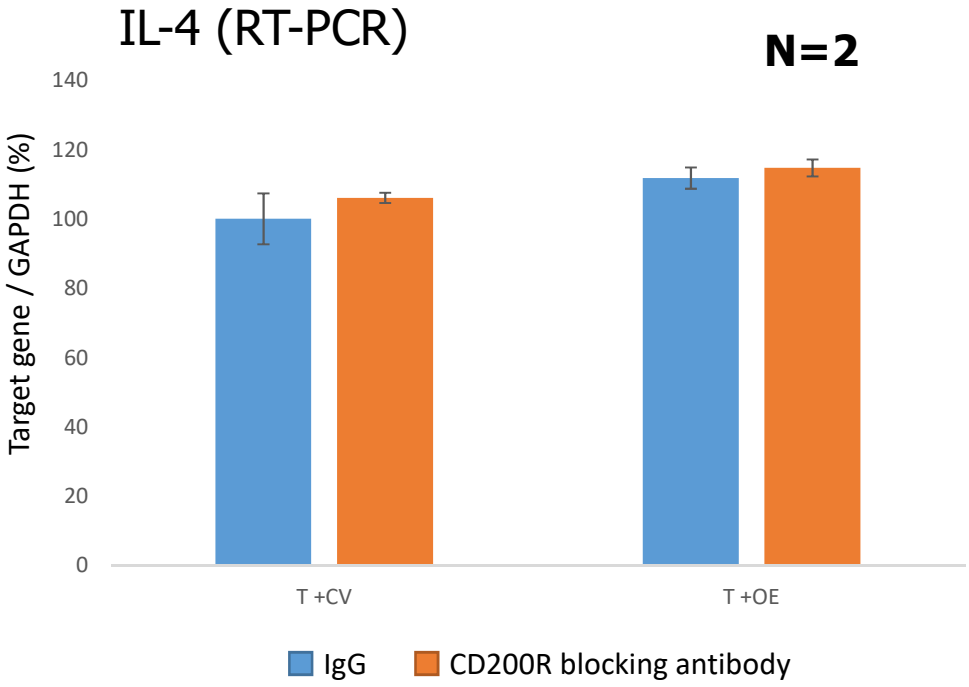

Figure 8.

A.

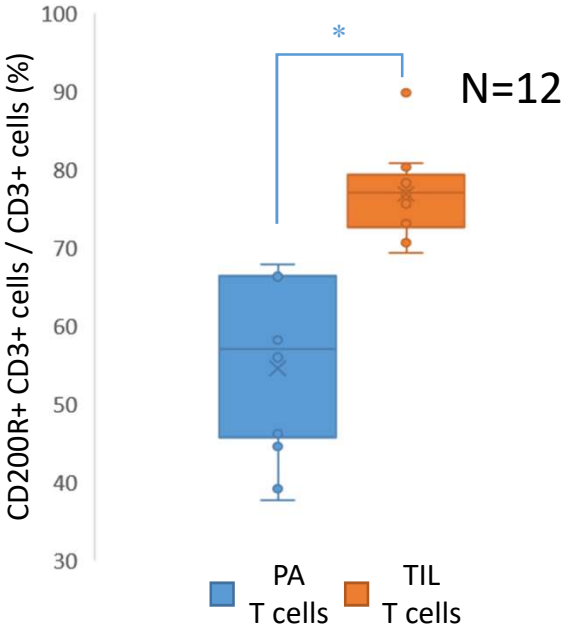
CD200R+ CD3+ cells / CD3+ cells (%)
100
90
80
70
60
50
40
30
*
N=12
PA
T cells
TIL
T cells

B.

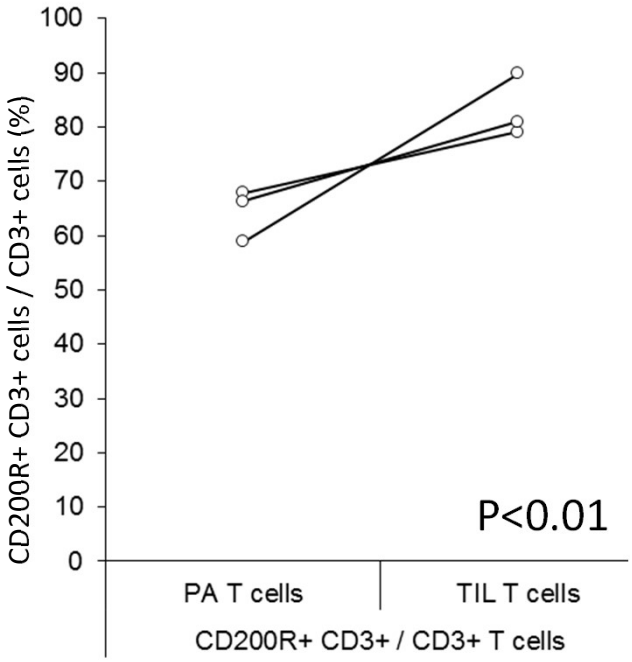
CD200R+ CD3+ cells / CD3+ cells (%)
100
90
80
70
60
50
40
30
20
10
0
P<0.01
PA T cells
TIL T cells
CD200R+ CD3+ / CD3+ T cells

Figure 9.

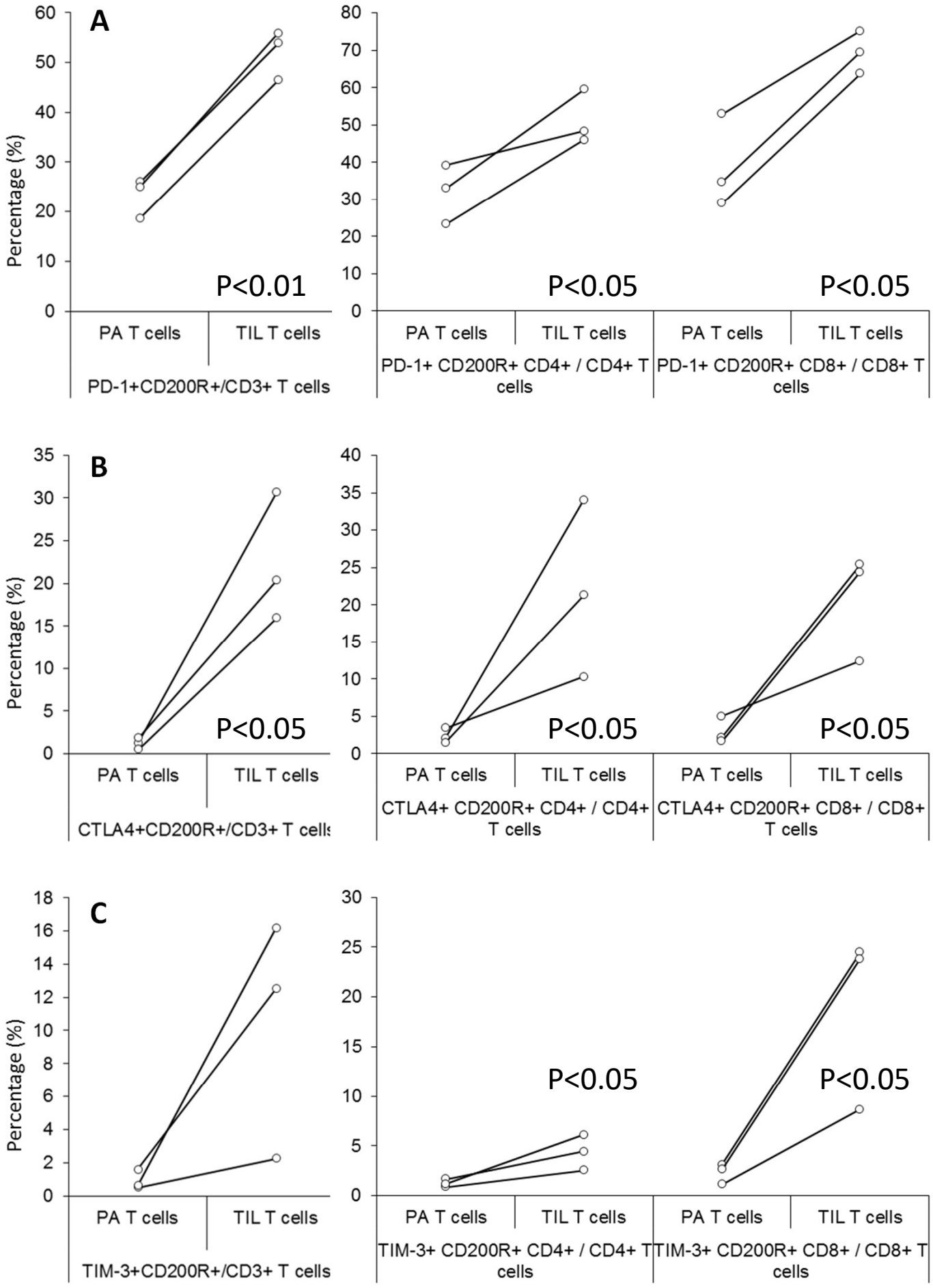
A
Percentage (%)
P<0.01
PA T cells
TIL T cells
PD-1+CD200R+/CD3+ T cells
P<0.05
P<0.05
PD-1+ CD200R+ CD4+ / CD4+ T cells
PD-1+ CD200R+ CD8+ / CD8+ T cells
B
P<0.05
CTLA4+CD200R+/CD3+ T cells
P<0.05
P<0.05
CTLA4+ CD200R+ CD4+ / CD4+ T cells
CTLA4+ CD200R+ CD8+ / CD8+ T cells
C
P<0.05
TIM-3+CD200R+/CD3+ T cells
P<0.05
P<0.05
TIM-3+ CD200R+ CD4+ / CD4+ T cells
TIM-3+ CD200R+ CD8+ / CD8+ T cells

Figure 10.

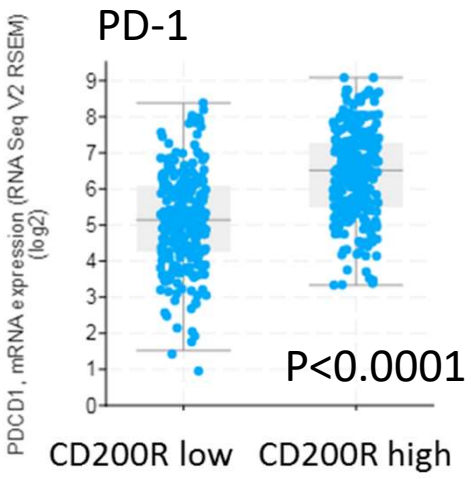
PD-1
PDCD1, mRNA expression (RNA Seq V2 RSEM) (log2)
P<0.0001
CD200R low
CD200R high

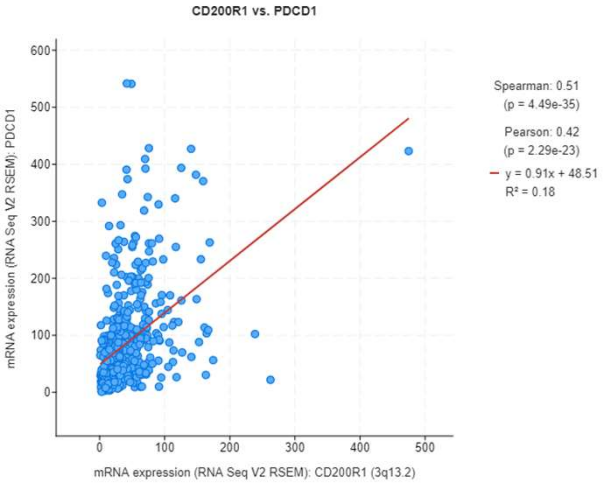
CD200R1 vs. PDCD1
mRNA expression (RNA Seq V2 RSEM): PDCD1
mRNA expression (RNA Seq V2 RSEM): CD200R1 (3q13.2)
Spearman: 0.51
(p = 4.49e-35)
Pearson: 0.42
(p = 2.29e-23)
y = 0.91x + 48.51
R² = 0.18

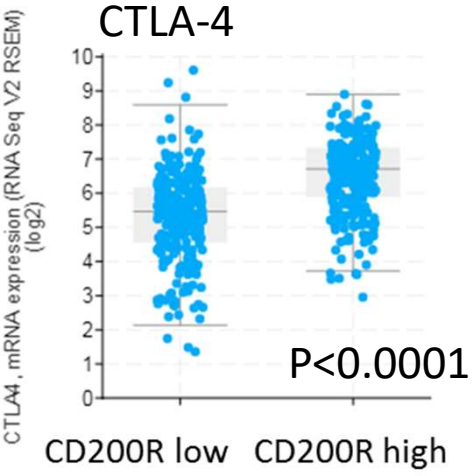
CTLA-4
CTLA4, mRNA expression (RNA Seq V2 RSEM) (log2)
P<0.0001
CD200R low
CD200R high

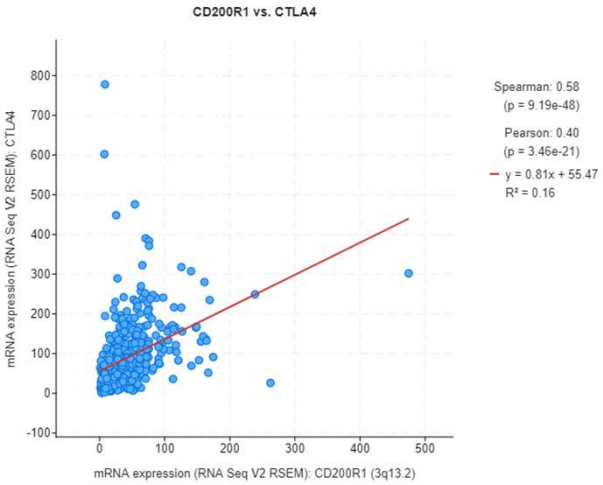
CD200R1 vs. CTLA4
mRNA expression (RNA Seq V2 RSEM): CTLA4
mRNA expression (RNA Seq V2 RSEM): CD200R1 (3q13.2)
Spearman: 0.58
(p = 9.19e-48)
Pearson: 0.40
(p = 3.46e-21)
y = 0.81x + 55.47
R² = 0.16

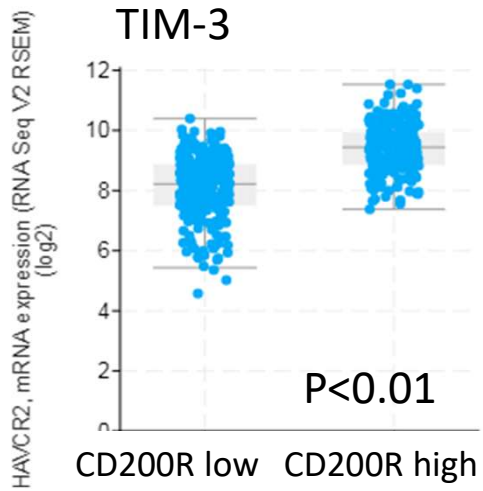
TIM-3
HAVCR2, mRNA expression (RNA Seq V2 RSEM) (log2)
P<0.01
CD200R low
CD200R high

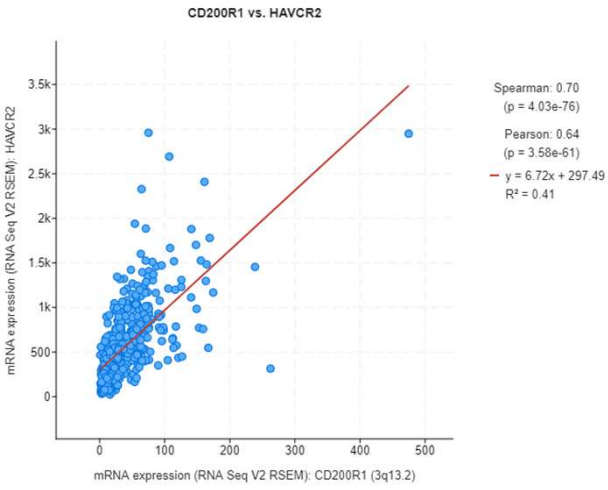
CD200R1 vs. HAVCR2
mRNA expression (RNA Seq V2 RSEM): HAVCR2
mRNA expression (RNA Seq V2 RSEM): CD200R1 (3q13.2)
Spearman: 0.70
(p = 4.03e-76)
Pearson: 0.64
(p = 3.58e-61)
y = 6.72x + 297.49
R² = 0.41

Figure 11.

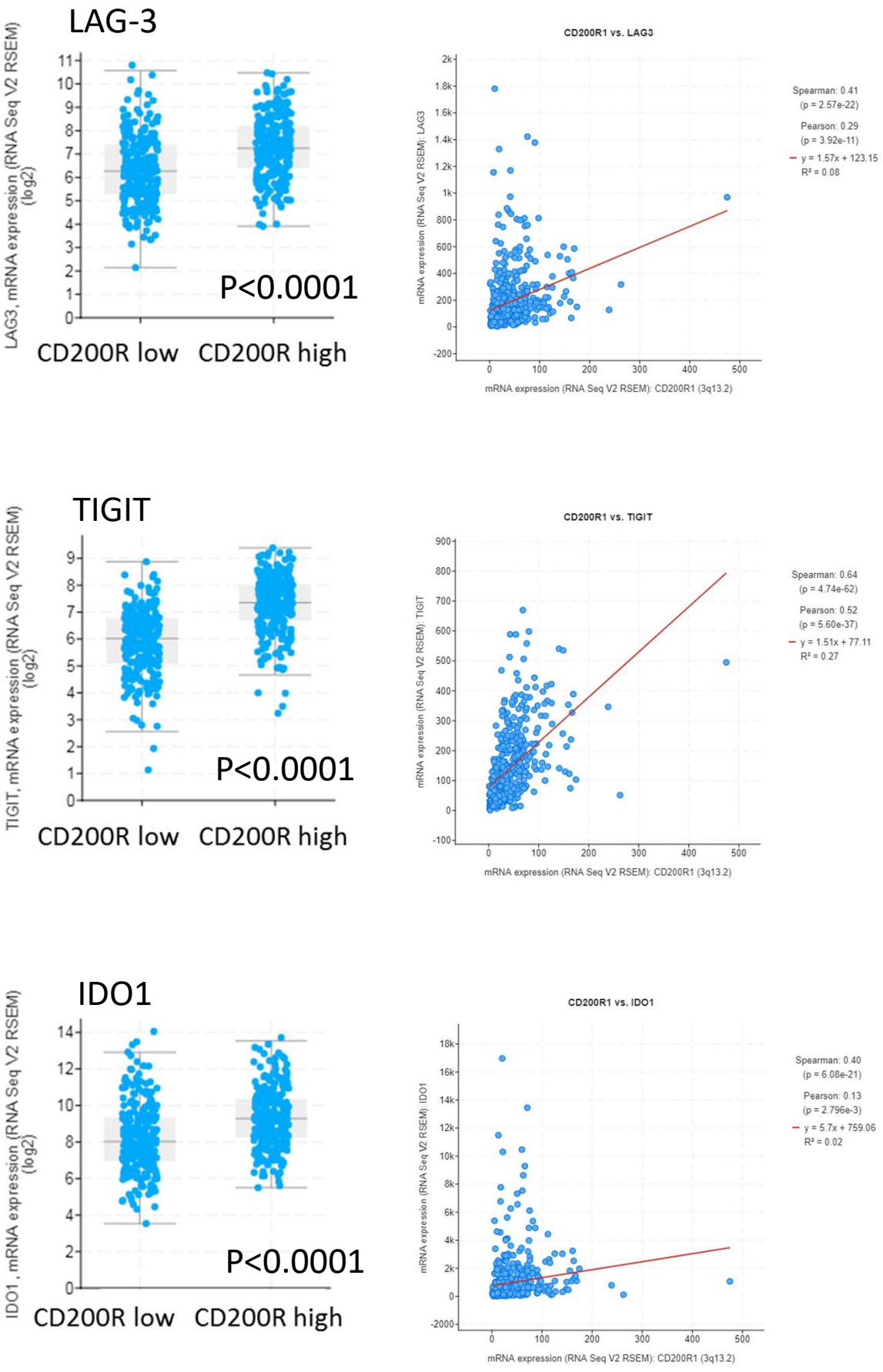
LAG-3
LAG3, mRNA expression (RNA Seq V2 RSEM) (log2)
P<0.0001
CD200R low
CD200R high
CD200R1 vs. LAG3
mRNA expression (RNA Seq V2 RSEM): LAG3
mRNA expression (RNA Seq V2 RSEM): CD200R1 (3q13.2)
Spearman: 0.41
(p = 2.57e-22)
Pearson: 0.29
(p = 3.92e-11)
y = 1.57x + 123.15
R² = 0.08
TIGIT
TIGIT, mRNA expression (RNA Seq V2 RSEM) (log2)
P<0.0001
CD200R low
CD200R high
CD200R1 vs. TIGIT
mRNA expression (RNA Seq V2 RSEM): TIGIT
mRNA expression (RNA Seq V2 RSEM): CD200R1 (3q13.2)
Spearman: 0.64
(p = 4.74e-62)
Pearson: 0.52
(p = 5.60e-37)
y = 1.51x + 77.11
R² = 0.27
IDO1
IDO1, mRNA expression (RNA Seq V2 RSEM) (log2)
P<0.0001
CD200R low
CD200R high
CD200R1 vs. IDO1
mRNA expression (RNA Seq V2 RSEM): IDO1
mRNA expression (RNA Seq V2 RSEM): CD200R1 (3q13.2)
Spearman: 0.40
(p = 6.08e-21)
Pearson: 0.13
(p = 2.796e-3)
y = 5.7x + 759.06
R² = 0.02

Supplementary Figure S1.

A.

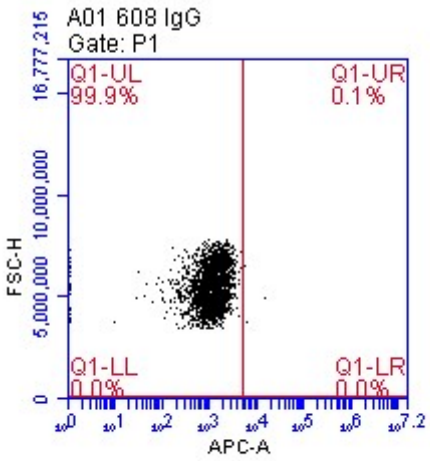

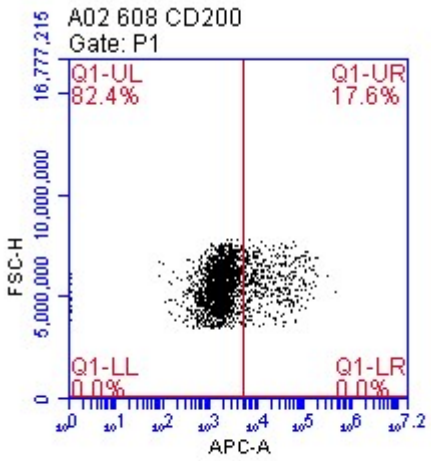

B.

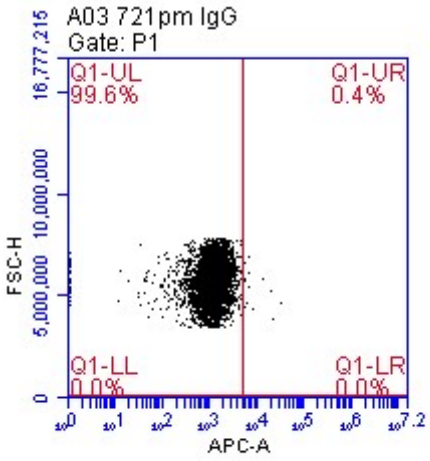

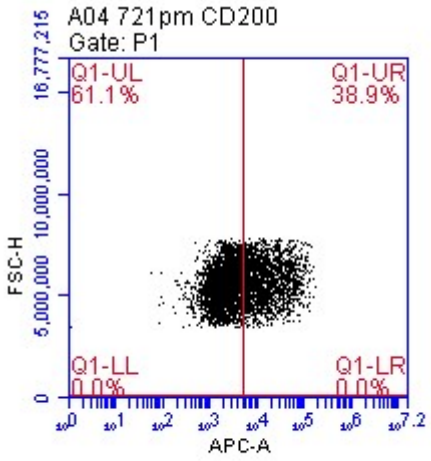

C.

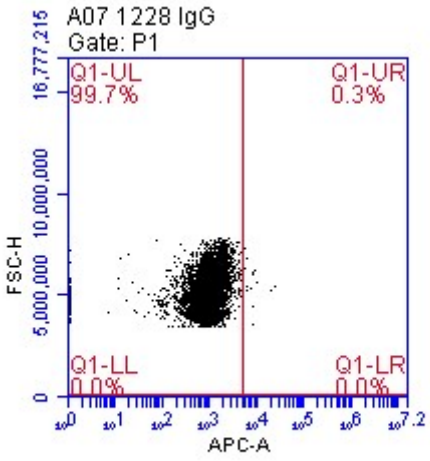

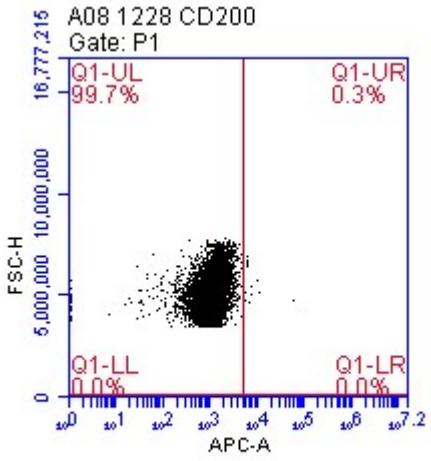

Supplementary Figure S2.

A.

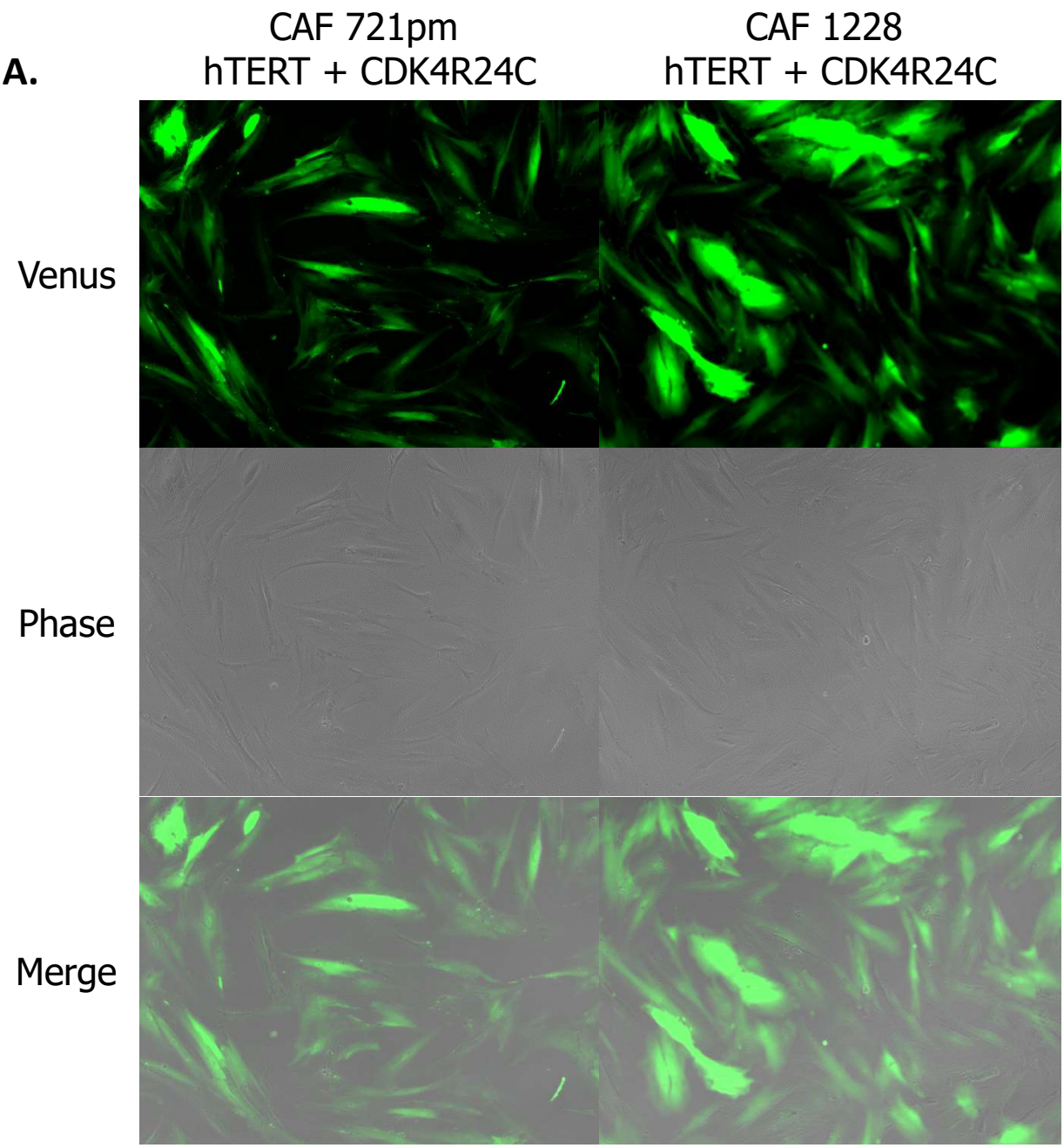

B.

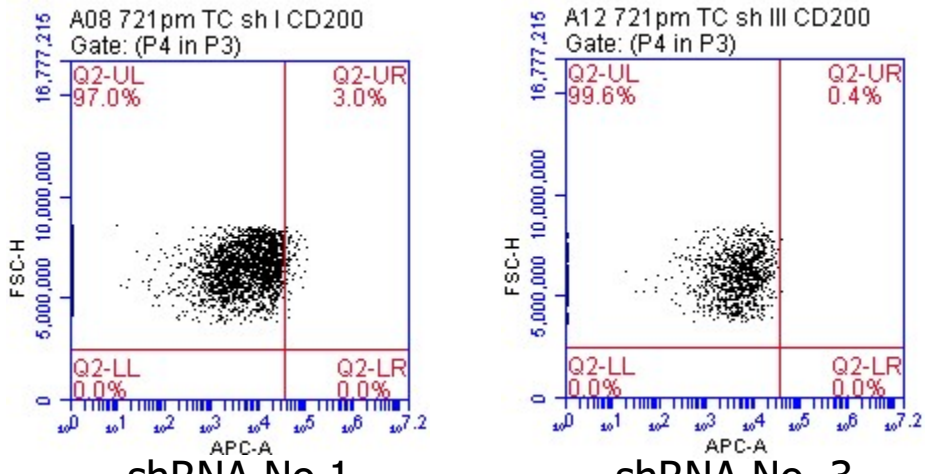

shRNA No.1 shRNA No. 3

Supplementary Figure S3.

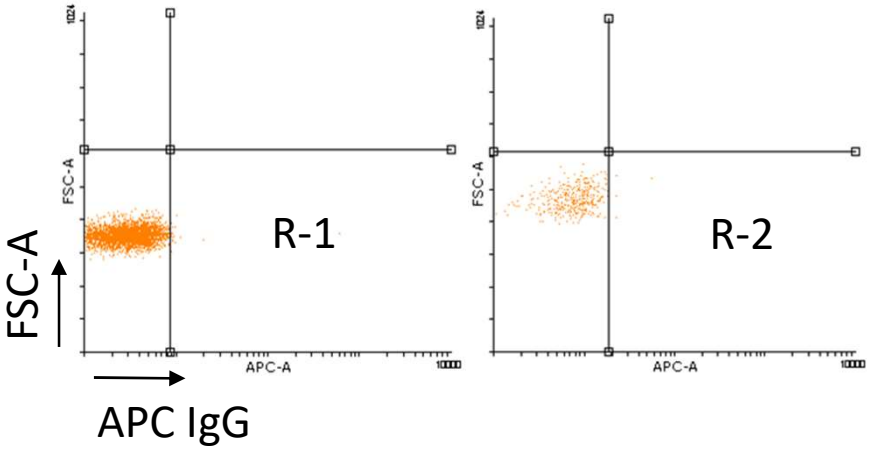

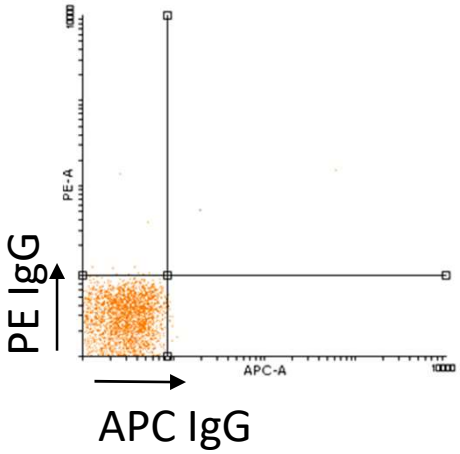

Supplementary Figure S4.

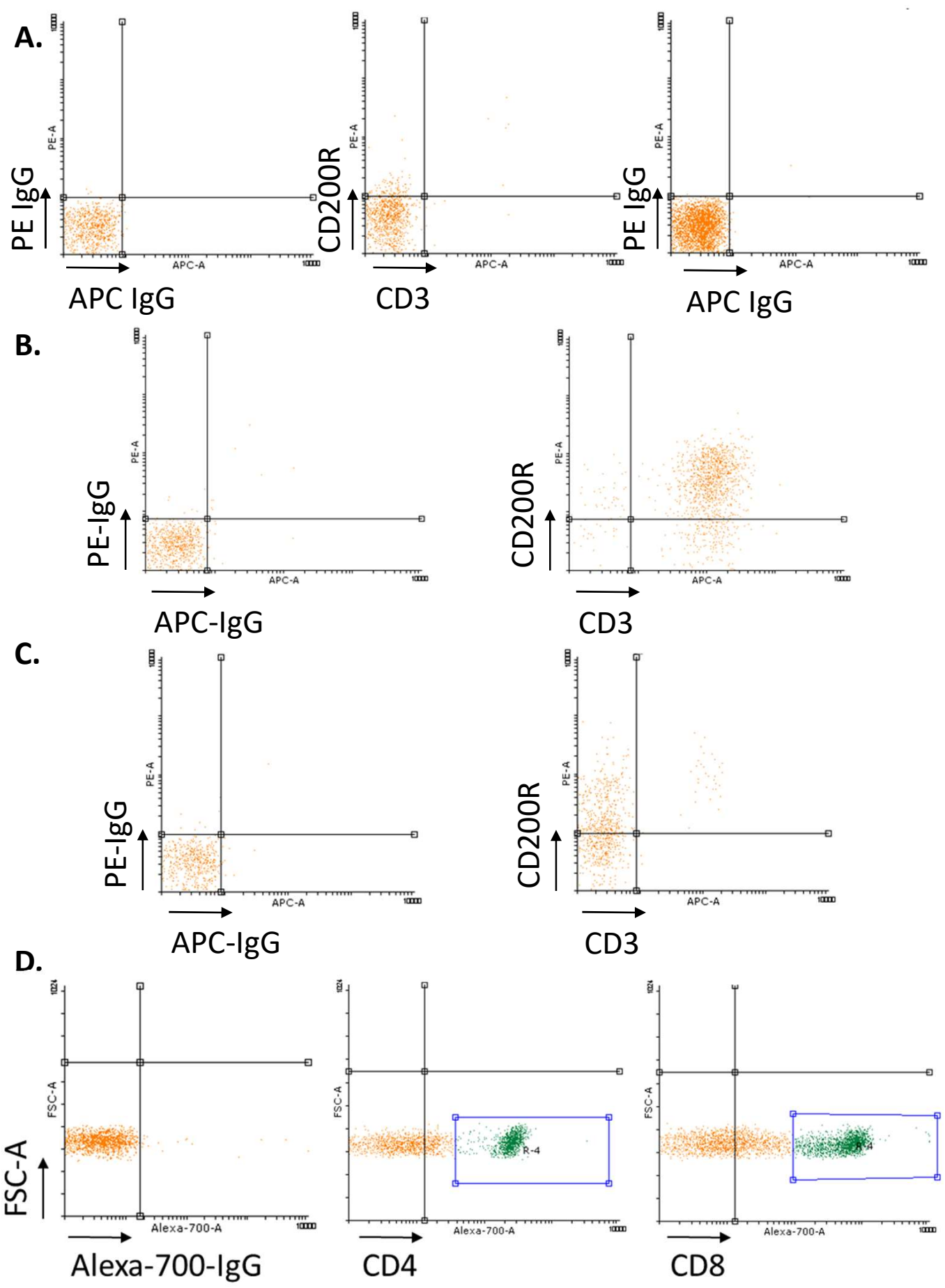

Supplementary Figure S5.

A.

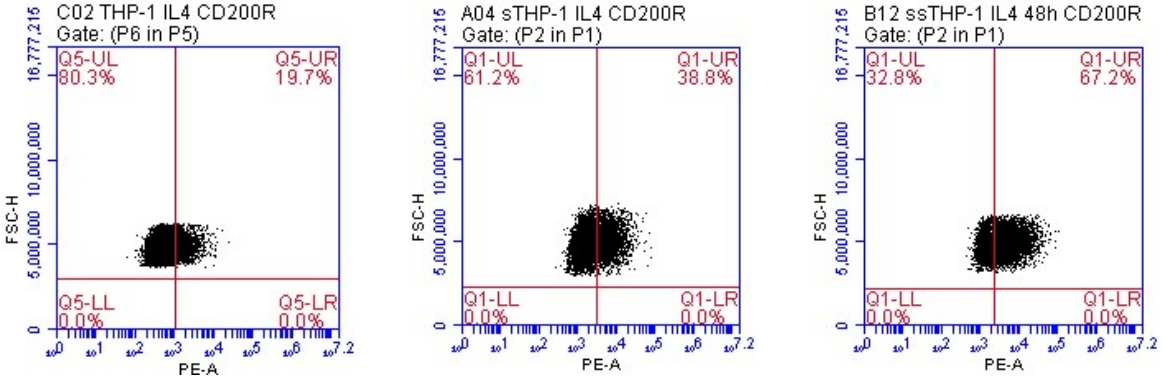

THP-1 IL4 48h CD200R Sorted THP-1 IL4 48h CD200R

B.

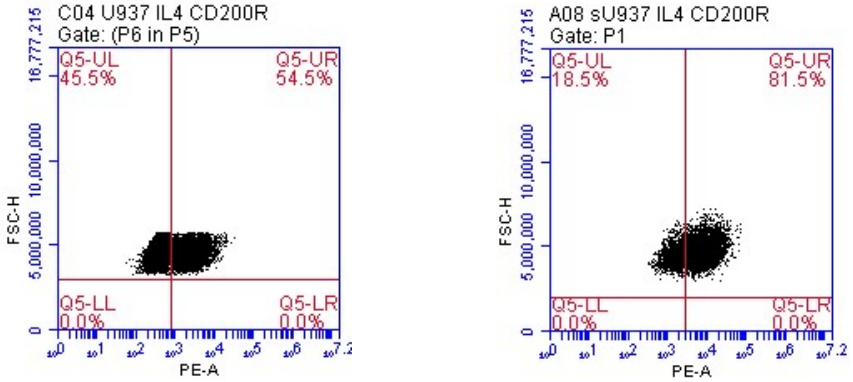

U937 IL-4 48h Sorted U937 IL-4 48h

C.

APC: CD200R

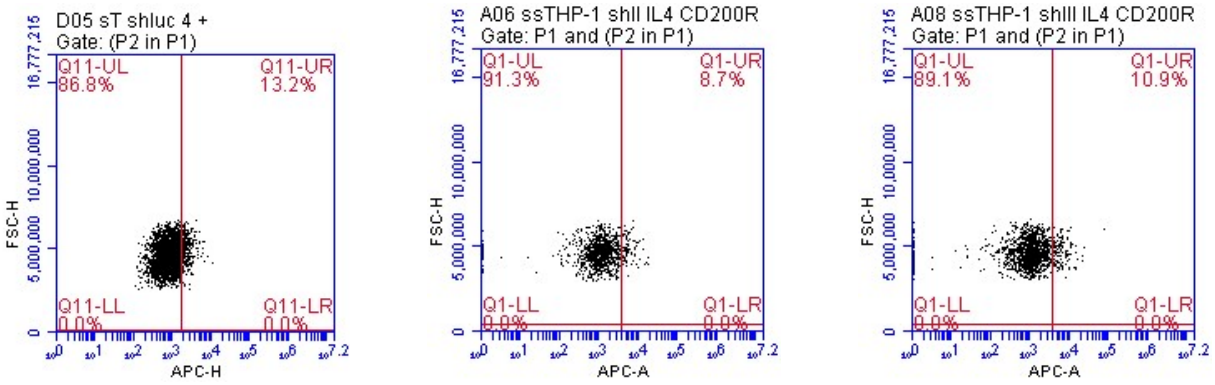

shRNA luc (con) shRNA No.2 shRNA No. 3

D.

IL-4 treating THP-1 20ng/ml

Seed CAFs (2.5×10^5 / 6 well)

Collect THP-1 (IL-4 48h)
Change medium
Add to CAFs (7.5×10^5 / 6 well).

Collect THP-1 cells
RNA extraction for PCR.

Supplementary Figure S6.

A.

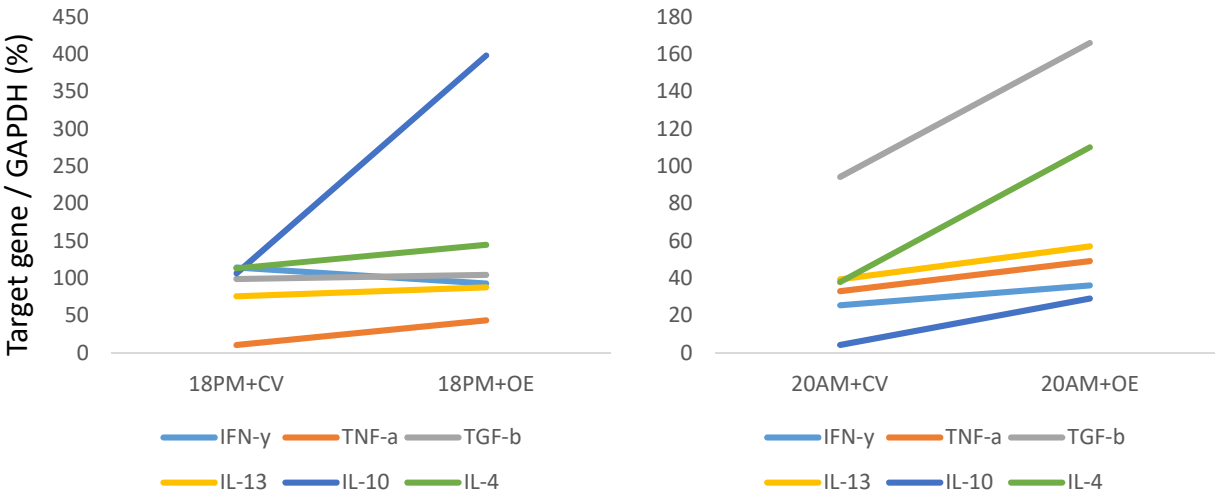

B.

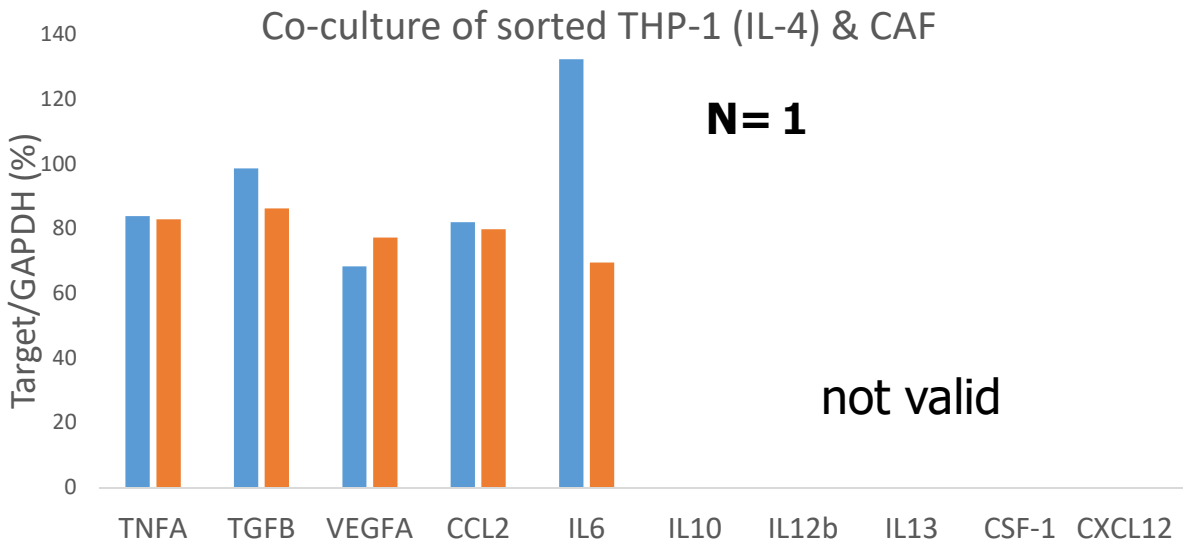

C.

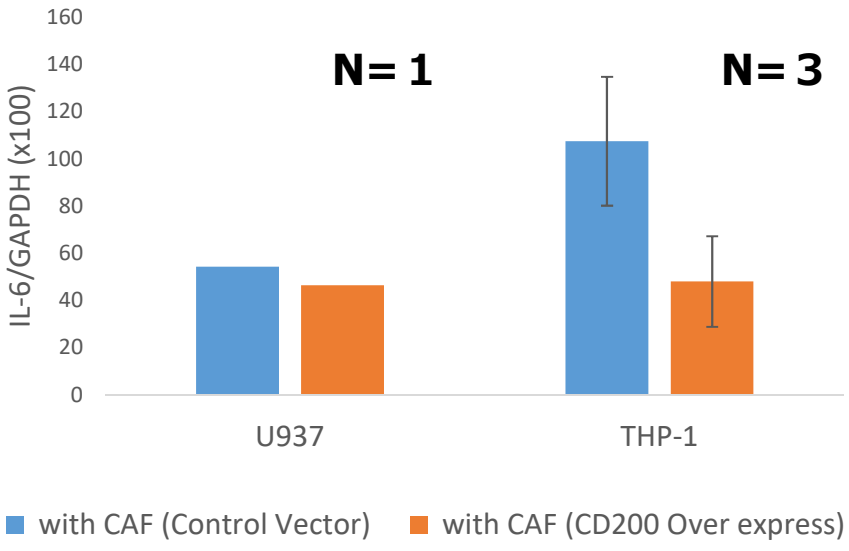

Supplementary Figure S7.

A.

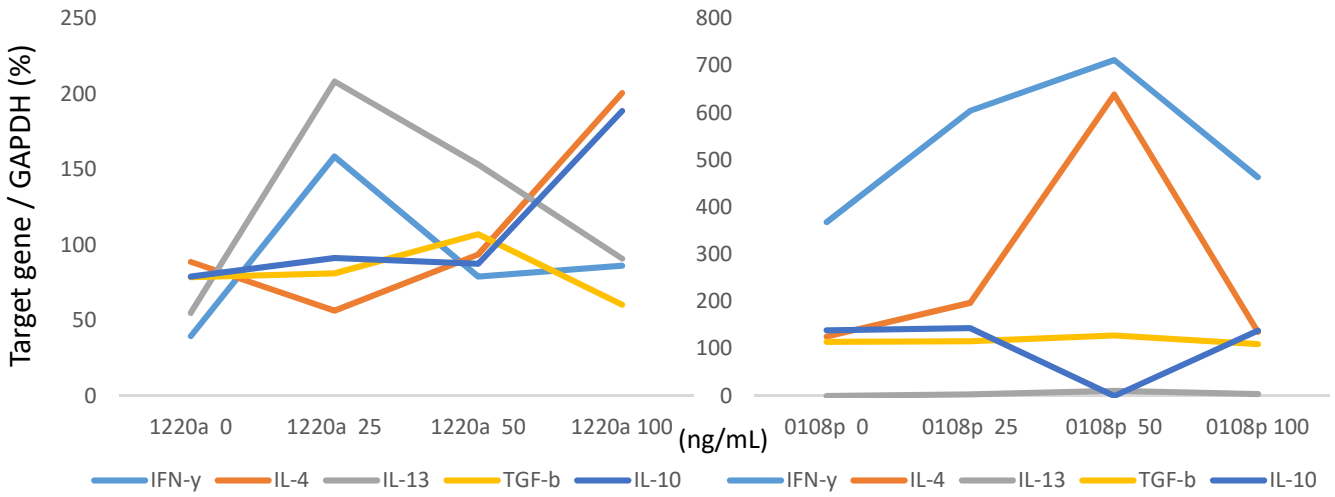

B.

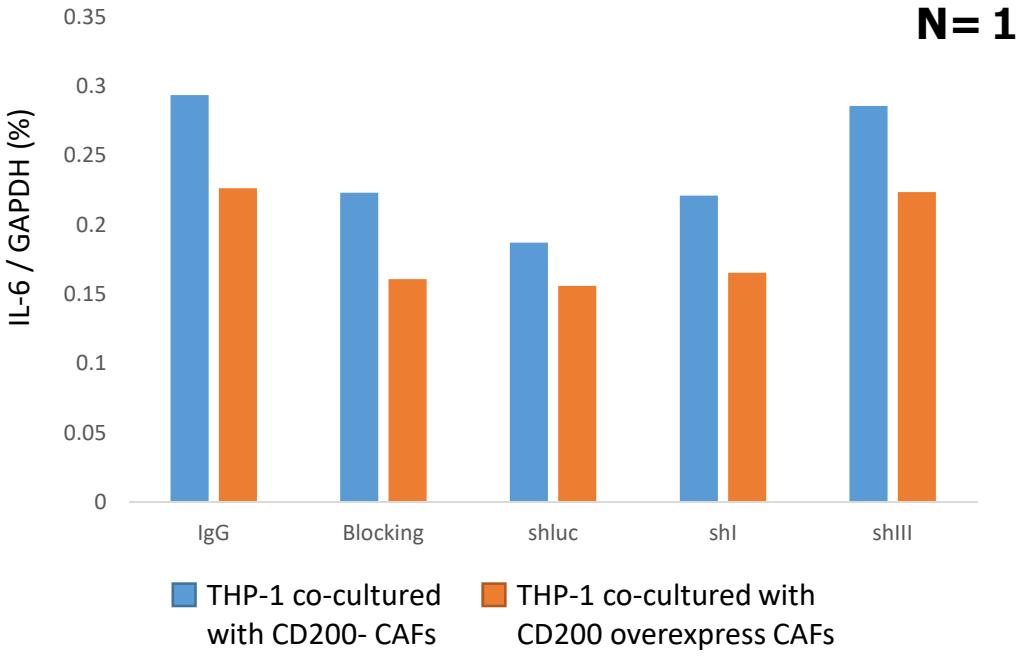

Supplementary Figure S8.

A.

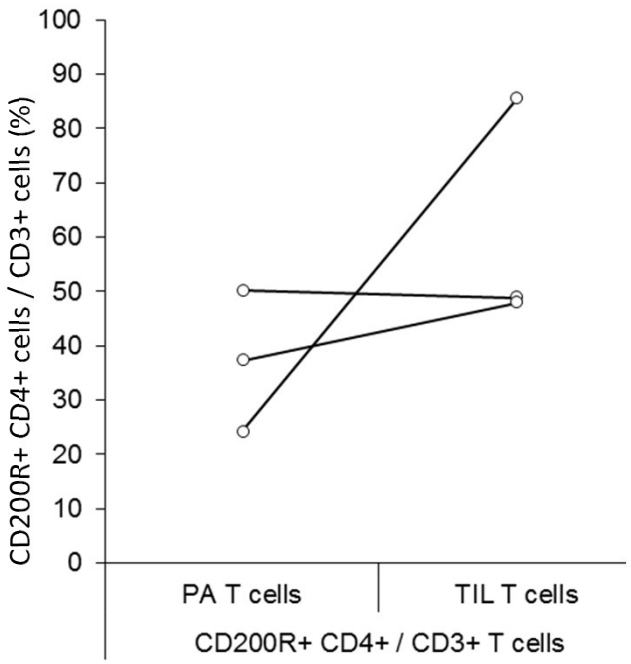

B.

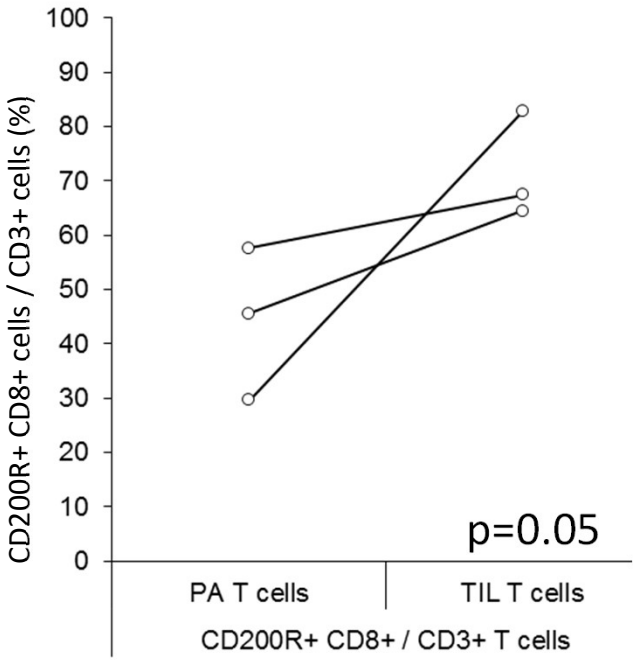

Supplementary Figure S9.

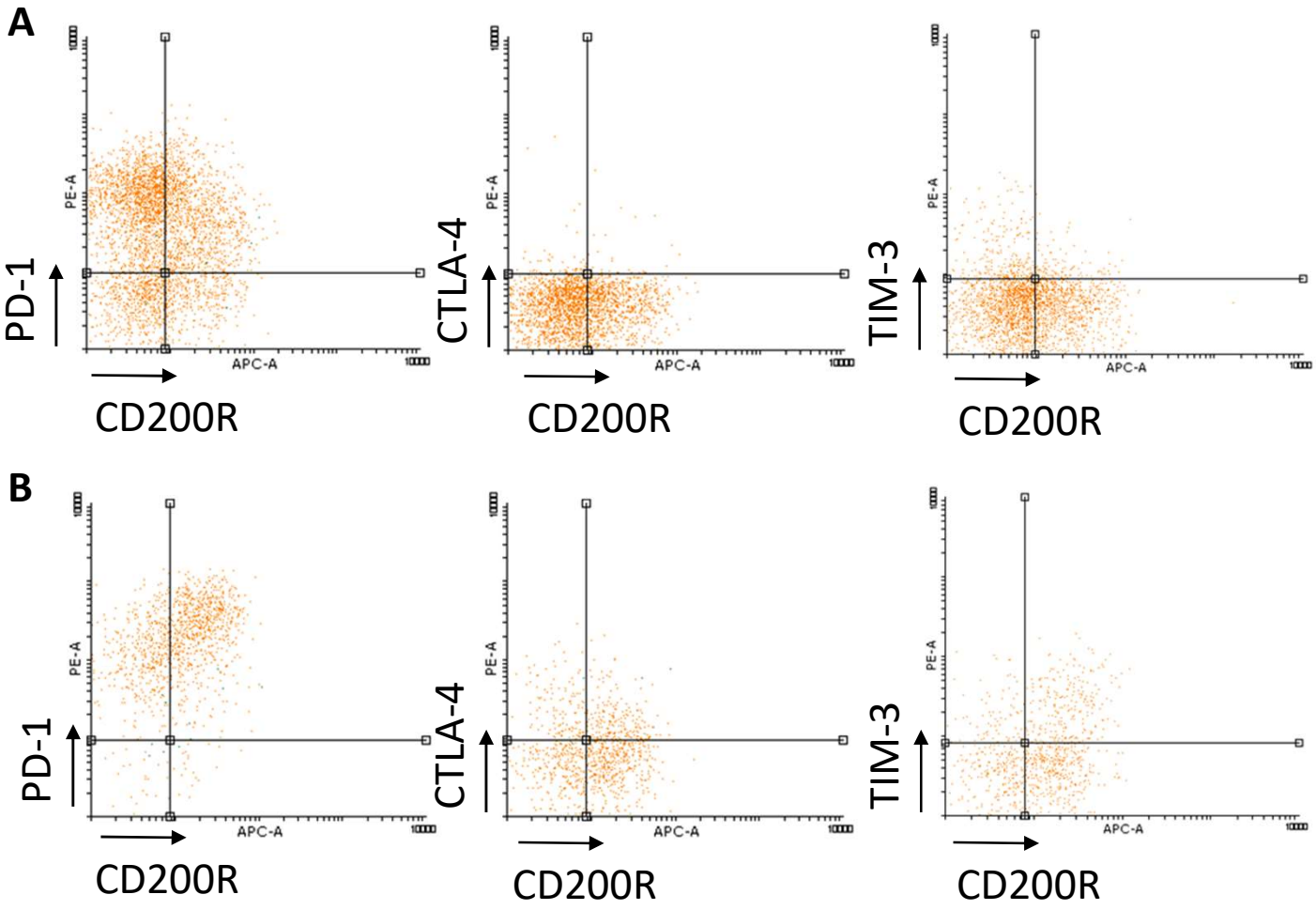

Supplementary Figure S10.

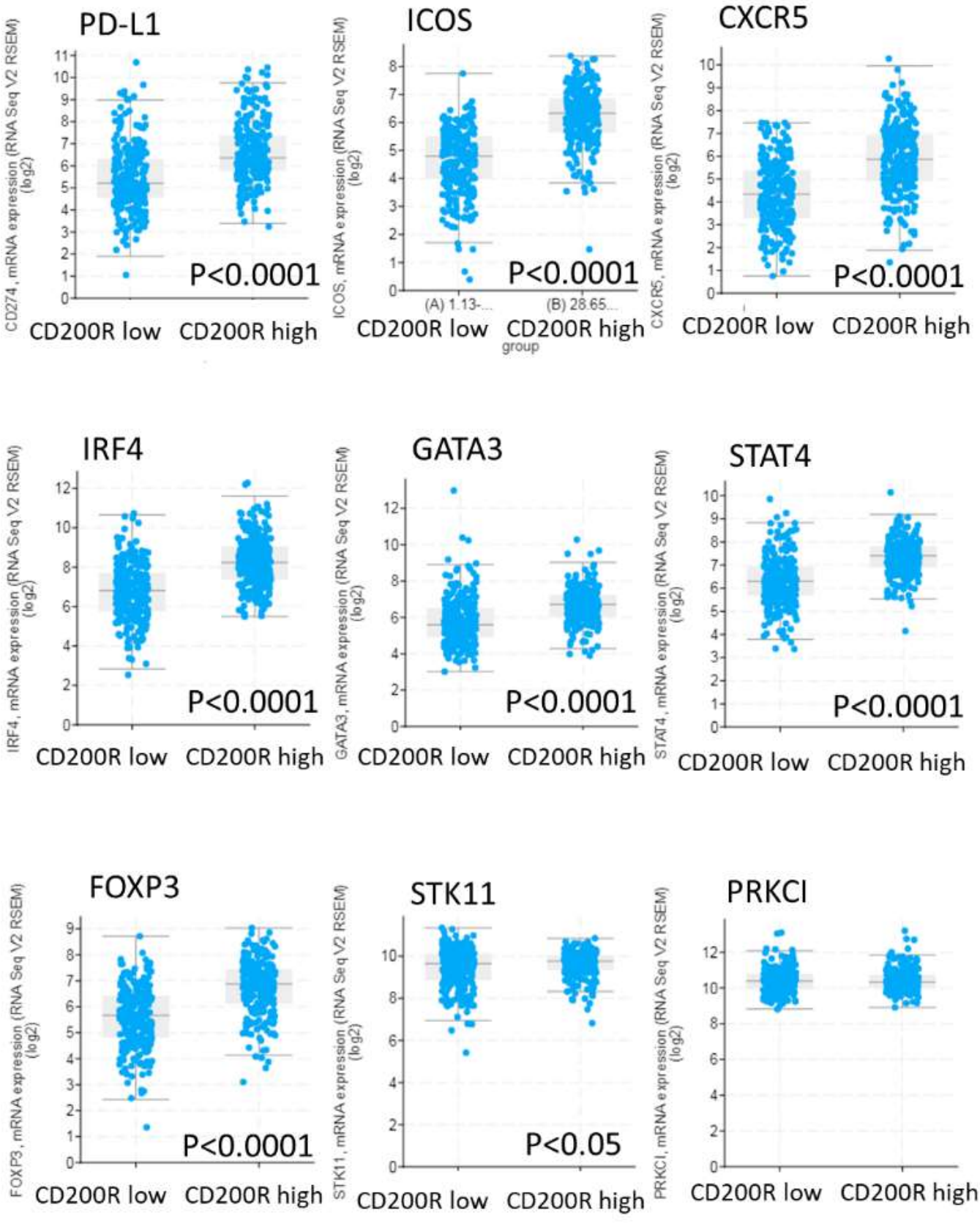

Supplementary Figure S11.

A.

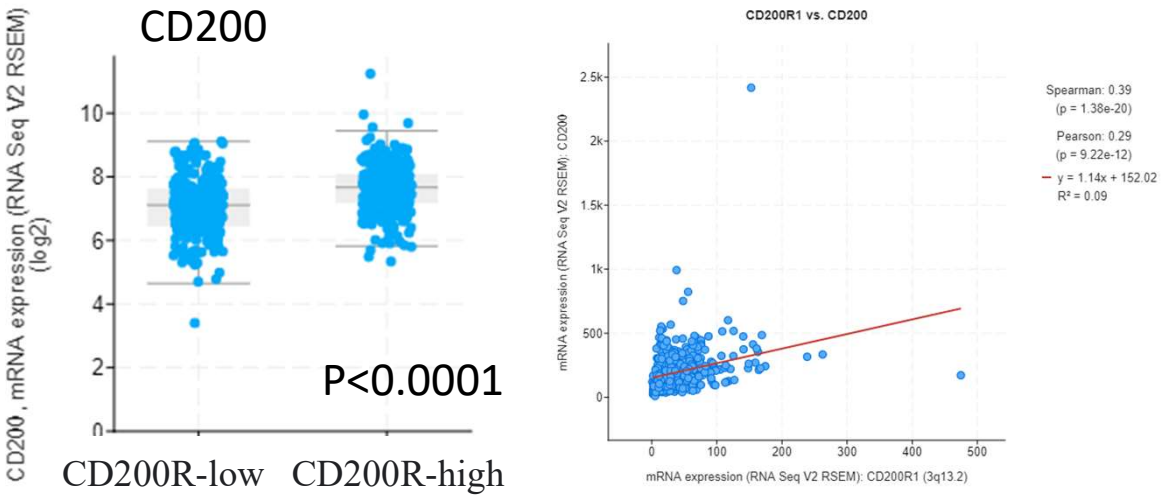

B.

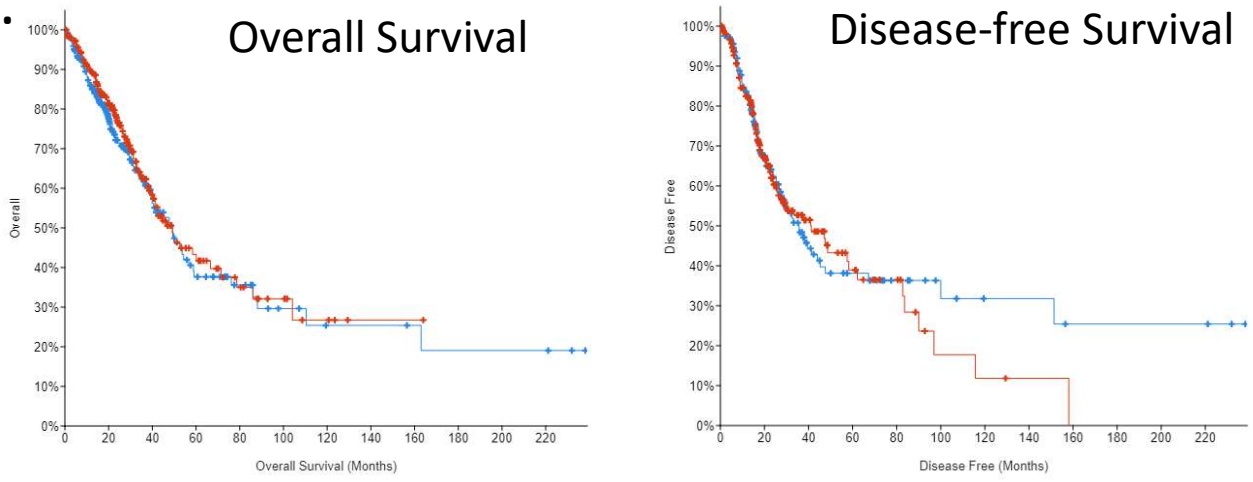

C.

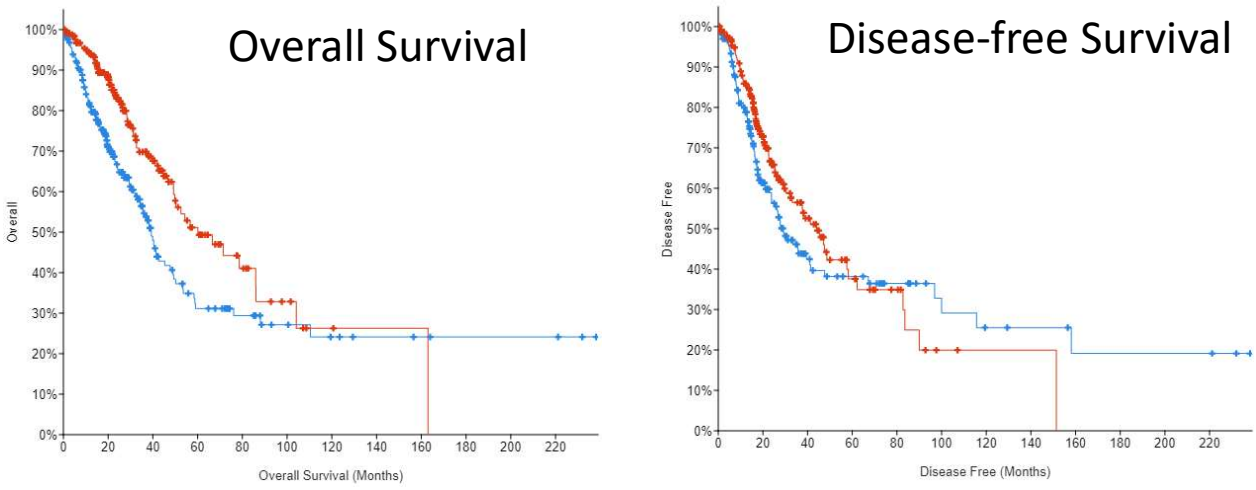

Supplementary Figure S12.

Destination vector

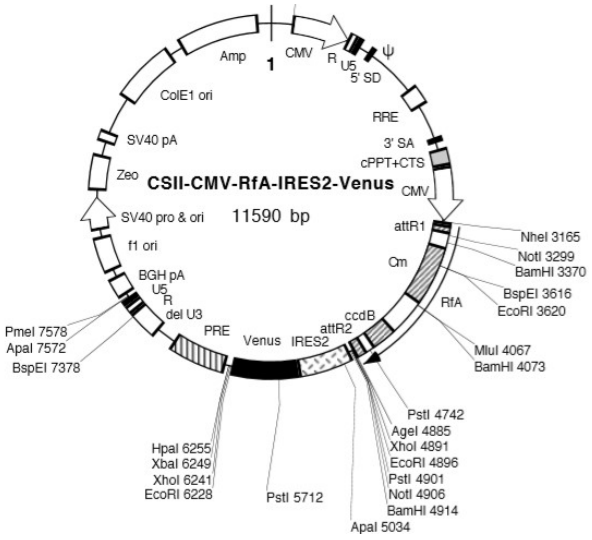

CSII-CMV-RfA-IRES2-Venus

*Venus: constitutively fluorescent protein

Amp: Ampicillin resistance

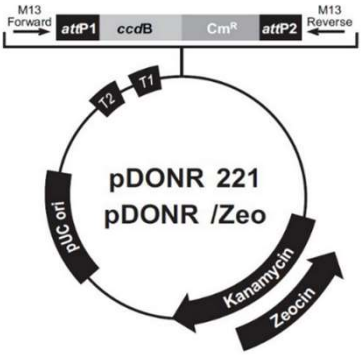

pDONR221-hTERT

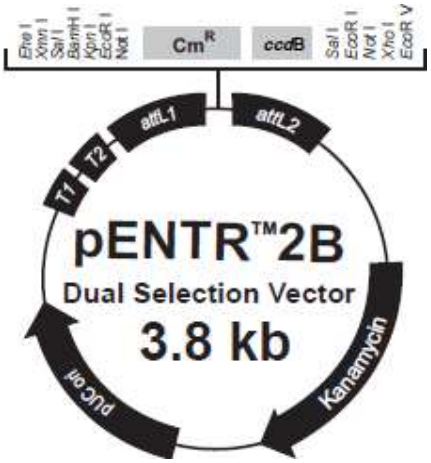

pENTER221-hCDK4R24C

Packaging vector

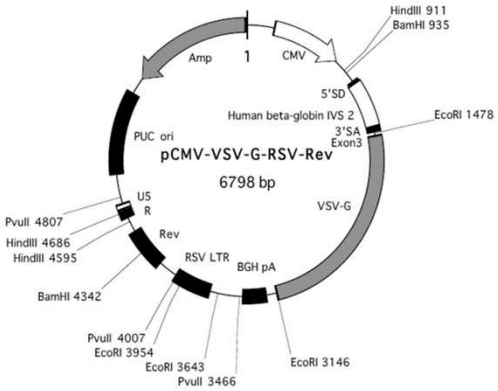

pCMV-VSV-G-RSV-Rev

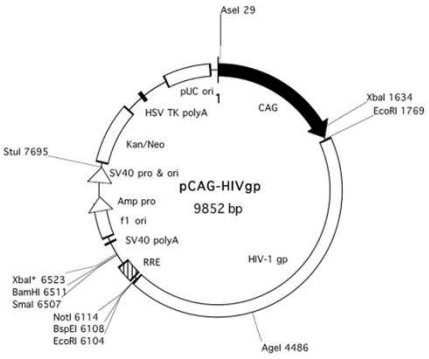

pCMV-HIV

Supplementary Table S1.

Antibody	Host	Experiment	Manufacturer	Reference no.
Recombinant IL-4	E. coli	stimulate THP-1 cells	Shenandoah Biotechnology, Inc.	100-09-5ug
Recombinant IL-2	Insect	T cell maintainance	BioLegend	589102
Anti CD3	Mouse	T cell amplification	BioLegend	317325
Anti CD28	Mouse	T cell amplification	BioLegend	302902
Recombinant CD200	293E cells	Functional assay	BioLegend	770004
CD200 Blocking antibody	Mouse	Functional assay	R&D Systems	MAB27243-100
CD200R Blocking antibody	Goat	Functional assay	R&D Systems	AF3414

Supplementary Table S2.

Luciferase sh
5’ - GATCCCC GTAAGGAGAGTCGTGCTTTAA ACGTGTGCTGTCCGT TTAAAGCATGATTCTCCTTGC TTTTT GGAAAT - 3’
3’ - GGG CATTCCTCTCAGCACGAAATT TGCACACGACAGGCA AATTTCGTACTAAGAGGAACG AAAAA CCTTTAGATC - 5
CD200R1 sh#1
5’ - GATCCCC GGAGACCAGCTGTATTGATGA ACGTGTGCTGTCCGT TCATCAGTACAGTTGGTTTCC TTTTT GGAAAT - 3’
3’ - GGG CCTCTGGTCGACATAACTACT TGCACACGACAGGCA AGTAGTCATGTCAACCAAAGG AAAAA CCTTTAGATC - 5
CD200R1 sh#2
5’ - GATCCCC GGAGACCAGCTGTATTGATGA ACGTGTGCTGTCCGT TCATCAGTACAGTTGGTTTCC TTTTT GGAAAT - 3’
3’ - GGG CCTCTGGTCGACATAACTACT TGCACACGACAGGCA AGTAGTCATGTCAACCAAAGG AAAAA CCTTTAGATC - 5
CD200R1 sh#3
5’ - GATCCCC GCGTCTGAGGTATTACAGAGT ACGTGTGCTGTCCGT ACTTTGTAATGCCTCAGATGC TTTTT GGAAAT - 3’
3’ - GGG CGCAGACTCCATAATGTCTCA TGCACACGACAGGCA TGAAACATTACGGAGTCTACG AAAAA CCTTTAGATC - 5

Supplementary Table S3.

Gene name	Forward	Reverse
hTERT	5‘ - ACGGTGTGCACCAACATCTACAA - 3'	5‘ - TCAGAGATGACGCGCAGGA - 3'
CDK4	5‘ - GCCTGGCCAGAATCTACAGCTAC - 3'	5‘ - GGTCGGCTTCAGAGTTTCCAC - 3'
CD200	5‘ - GTTTGGGTCATGGCAGCAGT - 3'	5‘ - CCATGTCACAATGAGGGCTTC - 3'
IFN-y	5‘ - CTTTAAAGATGACCAGAGCATCCAA - 3'	5‘ - GGCGACAGTTCAGCCATCAC - 3'
TNF-a	5‘ - TGTCTCAAGCTGCACGGACTC - 3'	5‘ - GAATGGTGTTCTGGAACCTGGA - 3'
TGF-β1	5' - AGCGACTCGCCAGAGTGGTTA - 3'	5' - GCAGTGTGTTATCCCTGCTGTCA - 3'
IL-4	5' - CTGTGCACCGAGTTGACCGTA - 3'	5' - AGCTGCTTGTGCCTGTGGAA - 3'
IL-6	5' - GCCAGAGCTGTGCAGATGAG - 3'	5' - TCAGCAGGCTGGCATTTG - 3'
IL-10	5‘ - GAGATGCCTTCAGCAGAGTGAAGA - 3'	5‘ - AAGGCTTGGCAACCCAGGTA - 3'
IL-12b	5‘ - GGAGCGAATGGGCATCTGT - 3'	5‘ - TGGGTCTATTCCGTTGTGTCTTTA - 3'
IL-13	5‘ - TCGAGAAGACCCAGAGGATG - 3'	5‘ - GGTCCTGTCTCTGCAAATAATGATG - 3'
VEGFA	5' - CATCCAATCGAGACCCTGGTG - 3'	5' - TTGGTGAGGTTTGATCCGCATA - 3'
CCL2	5‘ - GCTCATAGCAGCCACCTTCATTC - 3'	5‘ - GGACACTTGCTGCTGGTGATTC - 3'
CSF-1	5‘ - TAGCCACATGATTGGGAGTGGA - 3'	5‘ - CTCAAATGTAATTTGGCACGAGGTC - 3'
CXCL12	5‘ - AAGCCCGTCAGCCTGAGCTA - 3'	5‘ - GGGTCAATGCACACTTGTCTGTT - 3'
GAPDH	5' - GCACCGTCAAGGCTGAGAAC - 3'	5' - TGGTGAAGACGCCAGTGGA - 3'

Supplementary Table S4.

Antibody	Host	clone	Manufacturer	Reference number (Channel)
CD3	Mouse	UCHT1	BioLegend	300411 (APC)
CD14	Mouse	63D3	BioLegend	367117 (APC)
CD20	Mouse	2H7	BioLegend	302309 (APC)
CD4	Mouse	RPA-T4	BioLegend	300514 (APC), 300526 (Alexa Fluor® 700)
CD8a	Mouse	HIT8a	BioLegend	300911 (APC), 300919 (Alexa Fluor® 700)
CD200R	Mouse	OX-108	BioLegend	329306 (PE), 329307 (APC)
CD279 (PD-1)	Mouse	EH12.2 H7	BioLegend	329905 (PE)
CD152 (CTLA-4)	Mouse	L3D10	BioLegend	349905 (PE)
CD366 (TIM-3)	Mouse	F38-2E2	BioLegend	345005 (PE)
IgG1	Mouse κ Isotype Ctrl (FC)	MOPC-21	BioLegend	400112 (PE), 400122 (APC), 400143 (Alexa Fluor® 700)
IgG2b	Mouse κ Isotype Ctrl (FC)	MPC-11	BioLegend	400319 (APC)
APC Annexin V Apoptosis Detection Kit with PI			BioLegend	640932 (APC)